ADDIS ABABA UNIVERSITY

COLLEGE OF NATURAL AND COMPUTATIONAL SCIENCES

SCHOOL OF EARTH SCIENCES

IDENTIFICATION OF GROUNDWATER POTENTIAL ZONES BY USING RADAR AND OPTICAL REMOTE SENSING: A CASE STUDY OF KETAR WATERSHED, ETHIOPIA

By:

WONDIFRAW NIGUSSIE

GSR/5374/09

Adviser:

Dr. BINYAM TESFAW

Co-Adviser:

Dr. TILAHUN AZAGEGN

A Thesis submitted to

School of graduate studies of Addis Ababa University in Partial Fulfillment of the requirements for the Degree of Master of Science in

Remote Sensing and Geo-informatics

Addis Ababa, Ethiopia

May,2018

ADDIS ABABA UNIVERSITY

COLLEGE OF NATURAL AND COMPUTATIONAL SCIENCES

SCHOOL OF EARTH SCIENCES

IDENTIFICATION OF GROUNDWATER POTENTIAL ZONES BY USING RADAR AND OPTICAL REMOTE SENSING: A CASE STUDY OF KETAR WATERSHED, ETHIOPIA

By:

WONDIFRAW NIGUSSIE

GSR/5374/09

A Thesis submitted to

School of graduate studies of Addis Ababa University in Partial Fulfillment of the requirements for the Degree of Master of Science in

Remote Sensing and Geo-informatics

Addis Ababa, Ethiopia

May, 2018

Addis Ababa University

School of Graduate Studies

This is to certify that the thesis prepared by **Wondifraw Nigussie**, entitled: "Identification of Groundwater Potential Zones by Using RADAR and Optical Remote sensing: A case study of Ketar Watershed, Ethiopia" and submitted in partial fulfillment of the requirements for the degree of Master of Science in Remote sensing and Geo-informatics complies with the regulations of the University and meets the accepted standards with respect to the originality and quality.

Signed by the Examining Committee:

Examiner: Prof. Tenalem Ayenew Signature ____________ Date __________

Examiner: Dr. K. V. Suryabahagavan Signature ____________ Date __________

Advisor: Dr. Biniyam Tesfaw Signature ____________ Date __________

Co-Advisor: Dr. Tilahun Azagegn Signature ____________ Date ___________

Prof. Tenalem Ayenew

Chairperson

Acknowledgments

Before anything, I would like to thank my GOD who gave me full health, peace, knowledge and Wisdom to accomplish this thesis work.

My deepest feeling of gratitude goes to my advisor Dr. Binyam Tesfaw from the Natural and Computational Sciences, School of Earth Sciences, Addis Ababa University for his strong advice, and constant encouragement to complete this research work successfully. I never forget his admirable patience, work quality, and attractive spirit of friendship. I also express my appreciation to my co-advisor Dr. Tilahun Azagegn from the Natural and Computational Sciences, School of Earth Sciences, Addis Ababa University for his professional guidance, encouragement and patience during the research period. I would like to express my special and sincere thanks to my instructors Dr. Tesfaye Korme and Dr. K.V. Suryabhagavan who helped and support me during my thesis work.

I also thank Dilla University, for allowing me to pursue my postgraduate studies. I extend my gratitude to European Space Agency, Ethiopian National Metrological Agency, Oromia Water Works Design and Supervision Enterprise (OWWDSE), Ethiopian Geological survey and Central Statistical Agency for providing me necessary data to carry out my research work.

My appreciation extends to my friends who helped during the study includes Demsachew Yilma, Getu Tessema, Gashaw Tesfaw, and Getachew Haile. My deepest gratitude goes to my family, especially my mother Wolela Chekilie, who is my hero in my life. Last but not least, I would like to thank my classmates and all my bests who contribute during this study.

Contents Page

List of Tables

List of Figures

List of Appendices

Acronyms

AHP	Analytical Hierarchical Process
CR	Consistency Ratio
CRV	Central Rift Valley
CSA	Central Statistical Agency
dB	Decibel
DEM	Digital Elevation Model
DN	Digital Number
EC	European Commission
ERDAS	Earth Resource Data Analysis System
ESA	European Space Agency
ETM	Enhanced Thematic Mapper
EW	Extra Wide Swath
GIS	Geographic Information Science
GMES	Global Monitoring for Environment and Security
GPR	Ground Penetrating Radar
GWPZ	Groundwater Potential Zone
GRD	Ground Range Detection
HH	Horizontal transmission and Horizontal reception
HV	Horizontal transmission and Vertical reception

IDW	Inverse Distance Weight
IWS	Interferometric Wide Swath
LU/LC	Land-use/Landcover
MCDM	Multi-Criteria Decision Making
MER	Main Ethiopian Rift
NDVI	Normalized Difference Vegetation Index
OLI	Operational Land Imagery
OWWDSE	Oromia Water Works Design and Supervision Enterprise
RADAR	RAdio Detection And Ranging
RGB	Red, Green, Blue
RI	Random Index
SAR	Synthetic Aperture Radar
SM	Strip Map
SMC	Soil Moisture Content
SNAP	Sentinel Application Platform
SWIR	Short Wave Infrared
TM	Thematic Mapper
TOARB	Top of Atmospheric Reflectance Byte
VNIR	Visible and Near-Infrared
VV	Vertical transmission and Vertical reception
WLC	Weighted Linear Combination
WV	Wave

Abstract

Groundwater is a precious water resource in underground rocks that is very important for drinking, industrialization and irrigation. However, identifying the groundwater potential zones in certain areas of Ethiopia is still challenging in terms of time and cost for resolving water scarcity problems and the management of groundwater systems. Therefore, this study used integrated optical and RAdio Detection And Ranging (RADAR) remote sensing to identify groundwater potential zones in Ketar watershed, Ethiopia. The two high-resolution (10 m) sentinel families, Sentinel-1A (RADAR) and Sentinel-2A (optical) imageries were processed and used for thematic layer derivation. Digital Elevation Model (DEM) was generated from Sentinel-1A, which has the same resolution with the processed image and used for thematic layer preparation. These thematic layers were lineament density, soil moisture, land-use/land-cover, drainage density, slope and geomorphology. Archived secondary data were used to get geological units, soil texture and rainfall thematic layers. These nine layers were considered as factors, which have influence for groundwater occurrence and analyzed through GIS environment. Since all factors have no equal contribution for the occurrence of groundwater, weight assessment was done using Analytical Hierarchy Process (AHP) technique. The result from weight comparison shows that, geological unit, rainfall, soil texture, slope and lineament density were the dominant factors. These identified factors were reclassified based on standard criteria; and aggregated using Weighted Linear Combination. The result revealed the groundwater potential zones: very low (607.64 km^2), low (942.19 km^2), moderate (777.2 km^2), high (598.74 km^2) and very high (428.23 km^2). These zones were validated and the result shows that 0.93 correlation based on 43 existing data of boreholes, hand dug wells and springs. The outcome of this study emphasizes the importance of integrated optical and RADAR remote sensing in identifying potential groundwater zones to address the water scarcity problems.

Keywords: Groundwater Potential Zones, Ketar Watershed, Sentinel, Thematic layers, Analytical Hierarchy Process

CHAPTER ONE

1 INTRODUCTION

1.1 Background of the Study

Water is the most vital requirement for life and a life-supporting system to mankind. Within the hydrologic cycle, groundwater represents a major portion of the earth's water circulatory system. Groundwater is an important resource required for drinking, irrigation and industrialization purpose (Rather and Andrabi, 2012). Groundwater is a precious and the most widely distributed resource of the earth. Groundwater is contained in underground rocks, which contain and transmit water in economical rate generally referred to as aquifers (Bereket Bezabih, 2017). Groundwater flows very slowly in the subsurface towards points of discharge, including wells, springs, rivers, lakes, and the ocean.

There is now a strong consensus that climate change poses a fundamental challenge to the well-being of all countries, with the potential of being the harshest on countries already suffering from water scarcity (Kumar *et al*., 2016). The solution to minimize this problem is using groundwater which is one of the most valuable natural resources to support human health, economic development and ecological diversity (Barik, 2017). This makes groundwater to become an immensely important and dependable source of water supplies in all climatic regions due to several inherent qualities.

The increased demand and abstraction of groundwater resources is a cause for concern in sub-Saharan Africa. However, the importance of groundwater for socio-economic improvement of developing countries like Ethiopia cannot be overemphasized (Bereket Bezabih, 2017). The central rift valley of Ethiopia is one of the environmentally vulnerable areas (Jansen *et al*., 2007). According to Jansen *et al.* (2007), conversion of natural vegetations into agriculture land is increasing due to rapidly growing population and improper land management. The rapid growth of population increases land degradation and deforestation results to strong competing claims of land and water resources. Timely mapping and monitoring of the quantity and annual abstraction levels of groundwater resources are critical if sustainable groundwater resources management is to be fully achieved. Conventionally, groundwater mapping has been conducted based on field surveys that depend on geomorphic interpretation expertise and ancillary data analysis. Considering that these methods are costly, laborious and time-consuming makes remote sensing and geospatial data analysis a better alternative for mapping groundwater resources, given the imminent need of knowledge on the status of this resource (Mbulisi *et al*., 2015).

The spatial, spectral and temporal availability of data in remote sensing has a great importance for covering large and inaccessible areas within a short time. Due to this, remote sensing became an efficient way of assessing, monitoring and conserving groundwater resources. The different types of groundwater indicators can be classified into two groups as direct and indirect indicators. The direct indicators are related to groundwater establishments as recharge zones, discharge zones, soil moisture and vegetation. Indirect indicators could be associated with different rock and soil types, structures including fracture zones, landforms, and drainage characteristics. The various thematic layers generated using satellite data provides quick and useful baseline information on the parameters controlling the occurrence and movement of groundwater like land-use / land-cover (LU/LC), lineaments and geomorphology. These maps can be integrated with geology /lithology/, soils, slope, drainage, rainfall and other collateral data in a Geographic Information System (GIS) framework and can be analyzed by using logical conditions to derive groundwater potential zones (Rather and Andrabi, 2012). The implementation of GIS tools and remote sensing data for exploration of groundwater in an area with scarce water resources saves time and money (Kolawole *et al*., 2016).

Data from the Copernicus Program and in particular images from the Sentinel satellites together with other free and open access medium resolution satellite imagery would be used to detect the geological features of the surfaces through visual inspection and band ratios on multispectral data. The comparison of multi-temporal images, showing the environmental changes in the past years, will allow the identification of active geomorphological processes (Melis *et al*., 2017).

Lineaments are structural lines such as faults, which often represent zones of fracturing and increased secondary porosity and permeability, and therefore of enhanced groundwater occurrence and movement. In hard rock terrain, the storage and movement of groundwater are controlled by the secondary porosity that is the presence of lineaments and fractures. A lineament from remotely sensed data provides important information on subsurface fractures that may control the movement and storage of the groundwater (Tesfaye Tessema, 2015).

Synthetic Aperture RADAR (SAR) imagery is particularly suited for geological mapping primarily in tropical regions, because of the geological structure, surficial bedrock, and lineaments information it provides. The RADAR backscatter qualities are directly related to ground topography, dielectric properties, and surface roughness of the terrain being imaged. In addition, RADAR can acquire multiple images which can be used to provide stereoscopic viewing. Sentinel-1 is a SAR mission, providing continuous all-weather, day-and-night imagery at C-band (Center frequency: 5.405 GHz), operating in four exclusive imaging modes with different spatial resolutions and coverage (Liu, 2016).

Rainfall is the most dominant influencing factor in the groundwater potentiality of any area and is the major water source in the hydrological cycle (Ibrahim and Ahmed, 2016). In addition to rainfall, groundwater occurrence and its movement depend on the geological setting (Jhariya *et al*., 2016). Availability of multispectral remote sensing data cheaply and its higher spectral resolution compared to remote sensing data with higher spatial resolution has proved valuable for geological mapping exploitation and mineral mapping. This has benefited applications such as landslide quantification, fault pattern mapping, rock and lineament mapping especially with advanced remote sensing techniques and the use of shortwave infrared bands. The synoptic view of satellite imagery facilitates a better appreciation of geomorphology and helps in mapping of different landforms and their assemblages. Therefore, this research aims to delineate groundwater potential zones by using optical and RADAR remote sensing data in Ketar watershed, Ziway-Shala basin, Central Main Ethiopian Rift (MER).

1.2 Statement of the Problem

Water demand from Groundwater is radically increasing due to the immense pressure on population and urbanization, global impact due to climate and weather change, repetitive drought condition and lack of rainfall (Ibrahim-Bathis and Ahmed, 2016). Groundwater is the major source of drinking water and its use for irrigation is forecast to increase substantially to struggle growing food insecurity. However, there is little quantitative information on groundwater resources in a certain Ethiopia. Groundwater evaluation in Ethiopia has mostly conducted by surveying field, which is challenging to handle in terms of time and capitals (Abdul-Aziz Hussein *et al*., 2016). In Ketar watershed, the number of population increases from time to time and most of them use water for drinking and irrigation from Ketar river and its tributaries. Ketar river is the main river in the watershed area, which discharges water to Lake Ziway. However, due to climate change and ultimate use of irrigation, the amount of water in river decreases. This directly affects the amount and quality of Lake Ziway from time to time, which results to have a water scarcity. This also triggers additional problems in the surrounding society to fulfill their needs. Due to these, identification of groundwater potential zones is a better solution in order to manage and use the groundwater for different purposes and leads to sustainable management. Thus, mapping of groundwater consists in location of groundwater polygon boundaries. However, it has uncertainty in most cases that is caused mainly by difficulties while assigning the different thematic maps in the transition zone and locating the boundary between groundwater potential zones unless updating the data sources from currently available technologies and statistical validation has applied on it. Considering this, using remote sensing data for hydrogeological investigations and monitoring is the ability to generate information in spatial and temporal domain, which is very crucial for successful analysis, prediction and validation (Tessfaye Tesema, 2015). Therefore, in the study area, the identification of groundwater potential zones was investigated by integrating optical and microwave RADAR remote sensing data, which have a better spatial resolution (10 m).

1.3 Objectives of the Study

1.3.1 General Objective

The main aim of this study was identification of groundwater potential zones by using optical and microwave RADAR remote sensing in Ketar watershed, Ziway-Shala basin, Central Main Ethiopian Rift.

1.3.2 Specific Objectives

The specific objectives of this study were;

- Pre-processing and processing of optical and RADAR remote sensing data.
- Identifying the factors that govern groundwater potential zones.

- To investigate groundwater potential zones by geospatial techniques using Analytical Hierarchy Process.
- Validation of groundwater potential zone map.

14 Research questions

The following questions have been formulated to achieve the research objectives.

- What are the main processing stages for RADAR and optical remote sensing data?
- What are the factors that govern to identify groundwater potential?
- What areas are potential zones for groundwater occurrence?
- How accurate the identified groundwater zones map?

15 Significance of the study

Currently, groundwater is gaining more attention due to drought problem, rural water supply, and irrigation projects because apart from surface water sources, groundwater can provide year-round water availability and it is free from contamination relatively to other water sources such as surface water sources. Groundwater is an appropriate source of drinking water supply (reliable, clean and safe) because the potable water supply is a high priority need for urban and rural areas not only in the rift valley areas but also in many parts of Ethiopia. The output of this study will be used for government and non-government organizations to save their time and money while finding potential groundwater zone besides showing the effectiveness a groundwater potential zone mapping based on integrated optical and microwave RADAR remote sensing data processing for researchers.

16 Scope of the study

This study was focused on identification of groundwater potential zones by using integrated optical and RADAR remote sensing. The scope of the study was limited to the Ketar watershed in Ziway-Shala basin, Ethiopia.

17 Limitation of study

The lack of the whole groundwater inventory data information and unevenly distribution of point data were the problem of this research. The second limitation of the study was unevenly distribution of rain gage stations in the entire study area.

18 Thesis organization

This thesis was organized into six (6) chapters as follows:

Chapter one contains the background of the study and provides a brief overview of the overall study undertaken. It also provides information on the study and gives a highlight of the significance of the study as well as the goals and scope of the study. Chapter two emphasize on overview of water resources and geological setting of the study area. It also shows the application of GIS and remote sensing in groundwater zone identification and major factors that govern groundwater zone identification as well as previous works related to RADAR and optical remote sensing related to the study. Chapter three explains the datasets available as well as the method used to identify potential groundwater zones. Chapter four delivers information on the results. Chapter five contain discussion on the results related to previous works. Chapter six shows conclusion and recommendations.

CHAPTER TWO

2 LITERATURE REVIEW

2.1 Water Resource Assessment in the Ethiopian Central Rift Valley

The Central Ethiopian Rift valley (CRV) is characterized by a chain of lakes and wetlands with unique hydrological and ecological characteristics. An increasing claim on the precious freshwater resources was due to increasing population pressure and economic developments (Jansen *et al*., 2007). According to Jansen *et al*. (2007), water resources in the CRV encompasses by a chain of three large lakes (Ziway, Langano and Abijata) and streams that are spatially and temporally strongly interlinked. Lakes Ziway and Abijata are situated in a closed basin. This basin is referred to as the Ziway/Abijata catchment. Lake Ziway is the largest and the shallowest lake in the Central Main Ethiopian Rift (Tenalem Ayenew, 1998). The major incoming rivers to Lake Ziway are the Ketar river and Meki river. The Ketar river discharges the water from the eastern and south-eastern plateaus, and the Meki river discharges the runoff from the plateau west of Lake Ziway. The catchments of these two rivers cover an area of 5610 km^2 (Dagnachew Legesse *et al*., 2004). Groundwater and surface water interaction study of the Katar and Meki rivers based on discharge measurement indicates that these rivers lose a lot of water into the groundwater system within the rift floor. Hence discharge decreases downstream (Tenalem Ayenew, 1998). This is in part related to the existence of large open faults in the rift floor and adjacent escarpments.

The major source of irrigation water in the CRV is mainly from surface water, either by river diversion (44%) or from Lake Ziway (31%). Only 25% of the land is irrigated using groundwater through existing wells (Rodriguez De Francisco, 2008). Lake Ziway is the only lake, which is used for irrigation supply purpose (Tenalem Ayenew, 1998). Due to irrigation, water resources are currently over-exploited. Water extraction from Lake Abijata for the production of soda-ash seems relatively low compared to the extraction of water in upstream for irrigation and domestic use (Jansen *et al*., 2007). Existing groundwater abstractions are mostly from the unconsolidated alluvial and lake sediments that cover the volcanic rocks. Generally, these sediments have good hydraulic properties and are in direct contact with the lakes. The water divide of groundwater mirrors the surface water divide. There is no (significant) groundwater flow towards Lake Shala, Lake Abijata being the principal groundwater discharge location (Jansen *et al*., 2007).

2.2 Groundwater flow in the Ethiopian Central Rift Valley

According to Oromia Water Works Design and Supervision Enterprise (OWWDSE) (2016), groundwater flows to the rift floor from the highlands. This indicates that there is a topographic driven process at sub-regional scale. However, in the rift groundwater flow is strongly controlled by geological structures (OWWDSE, 2016). For instance, east of Lake Ziway much of the groundwater flows through large faults towards Lake Langano sub-basin following the faults-oriented N-S parallel and sub-parallel to the axis of the Ethiopian rift in the area. In the same locality, there are E-W running faults. These areas have been studied by the geophysicists in OWWDSE project. The result displays that these faults act as local conduits for the flow of large groundwater into Lake Ziway. These areas are found to be good groundwater localizers with better water quality.

2.3 Geological setting of Main Ethiopian Rift Valley

The Ethiopian geology contains a mixture of ancient crystalline basement rocks, volcanic rocks associated with the East African Rift system and sediments of various ages (British Geological Survey, 2001). The Main Ethiopian Rift (MER) is a part of the great African continental rift which is divided geographically into three sectors; Northern, central and southern (Tesfaye Korme, 1999). The geologic and geomorphic features observed in the region of Central Main Ethiopian Rift (CMER) are the results of Cenozoic volcano-tectonic and sedimentary processes (Tenalem Ayenew, 1998). The topography of central part of the MER is characterized by intensively faulted blocks with steep scarps forming local horst and graben structures (Tesfaye Korme, 1999). The MER represents a complex hydrogeologic setting composed of volcanic rocks of different type and age that are laterally discontinuous and intersected by faults (Abraham Mechal, 2016). An isolated block of Precambrian basement rocks and Mesozoic sediments is exposed at Kella along the western margin of the (CMER), surrounded by Tertiary to Quaternary volcanic rocks. The MER is a roughly NE-oriented segment of the East African Rift system, which extends from the Afar to the Kenya Rift. It has commonly been suggested that rift propagation in the MER progressed northwards (Wolfenden *et al*., 2004). Tertiary to

Quaternary volcanic are rocks exposed in the MER, apart from minor fluvial-lacustrine sediments, mostly of Quaternary age, that were deposited on the rift floor. One exception is an outcrop of Precambrian crystalline rocks covered by Mesozoic sediments at the base of the Guraghe escarpment, near the village of Kella about 80 km south-west of Addis Ababa. The areas around Lake Ziway and Lake Abijata predominantly consist of volcanic rocks associated with the rift system and sediments of various ages. The rift, the mountains, and plateaus flanking the rift valley are composed of volcanic rocks, with alkaline lavas, ashes and ignimbrites, mainly of tertiary and younger age. The volcanic rocks are silica-rich, including much ash and pumice (British Geological Survey, 2001). The sediments covering the volcanic rocks in the rift are mixed deposits of sandstone, limestone, and silts, with frequent occurrences of evaporite minerals. In addition, recent (Quaternary) unconsolidated alluvial and lake sediments are present (British Geological Survey, 2001). These unconsolidated sediments have good hydraulic properties and allow for high groundwater abstraction rates.

2.4 Major factors that govern Groundwater occurrence

Many studies were used GIS and remote sensing to study the groundwater potential of their region of interest. These papers have included thematic layers of rainfall, soil type, slope, lithology, geomorphology, LU/LC, lineaments and drainage density, although the minimum number of factors and the mechanism of assigning weight to these factors show variability. (Semere and Quiel, 2006; Oh, 2010; Rather and Andrabi, 2012; Kumer and Dev, 2014; Waikar and Nilawar, 2014; Abdul-Aziz Hussein *et al*., 2016; Ibrahim-Bathis and Ahmed, 2016; Jhariya *et al*., 2016; Kumar *et al*., 2016; Bari *et al*., 2017; Pinto *et al*., 2017). These studies were applied in various terrain and geologic formations. Some studies have applied probabilistic models such as multi-criteria decision analysis and weights-of-evidence modeling for groundwater potential mapping. Other studies have used personal judgments or local information to assign weight to different thematic layers and their features (Oh, 2011).

2.5 Application of GIS and Remote sensing in Groundwater Zone Identification

Groundwater potential zones are demarked with the help of remote sensing and GIS techniques. Conventional groundwater exploration methods such as geophysical investigations deliver higher quality results of varied scale, tend to be time consuming and expensive endeavors. The use of remotely sensed data and GIS opens up the possibility to harness information of vast spatial and temporal scale, analyze, and manage it efficiently (Bereket Bezabih, 2017). Remote sensing is a method which is used for identification of groundwater occurrence by interpreting lithology and structure (Moore, 1982). Remotely sensed surface indicators of groundwater provide useful data where practical classical alternatives are not available. Integrated remote sensing and GIS are widely used in groundwater mapping. Locating potential groundwater targets is becoming more convenient, cost-effective than invasive methods and efficient with the advent of a number of satellite imagery. The nature of remote sensing-based groundwater exploration is to delineate all possible features connected with localization of groundwater (Elbeih, 2015). Current methods for analyzing remote sensing data to delineate fractures and discontinuities in hard-rock terrains could be used to improve water-well sitting strategies. Groundwater recharge and discharge zones may be detected using satellite remote sensing techniques that enhance temperature, vegetation, and water content variations (Alonso-Contes, 2011).

2.6 Microwave Remote sensing for Groundwater Zone Identification

A remote sensing, either airborne or spaceborne using microwave radiation with a wavelength from about 1centi meters to 1metres that enables observation in all weather conditions without restriction by cloud or rain is a microwave remote sensing. RADAR is the common microwave remote sensing technology, which is an imaging active microwave sensor. The RADAR transmits a microwave (radio) signal towards the target and detects the backscattered portion of the signal (CCRS, 2013). SAR is an active microwave remote sensing instrument which can provide high-resolution images of the Earth's surface during both at day and night and virtually under all- weather conditions (Sanyal and Lu, 2004). SAR data offers a useful starting point for groundwater resource management decisions because of RADAR waves penetrate sand to reveal the courses of ancient rivers below today's surface (Robinson, 2007). SAR data are very useful for hydrological studies because the dielectric properties of materials are generally dependent on the amount of liquid water in the material, and this affects the strength of the radar backscatter, alpha naught ($\alpha°$). The ability of microwaves to penetrate the surface of many materials often permits analysis of subsurface properties. Further, SAR sensors can image the Earth through both clouds and darkness which enables dynamic hydrological events, e.g. floods, to be captured (Hall, 1996). The Ground Penetrating Radar (GPR) technique successfully yielded quantitative information about water table change, and the hydraulic properties could be estimated by combining GPR data and hydrogeologic data. GPR profiles show consistency by locating the antenna position accurately. The groundwater table change could be quantitatively estimated by comparing the two sets of GPR data acquired under different conditions. Quantitative information extracted from the GPR data indicates that GPR is a good tool for estimating the hydraulic properties of the aquifer (Zhu *et al*., 2009).

2.7 Soil Moisture Estimation Using Microwave Remote sensing

The theoretical basis for measuring soil moisture by microwave techniques is based on the large contrast between the dielectric properties of liquid water and of dry soil. Variables that affect the measurement of soil moisture includes Soil texture, surface roughness, vegetation effects and instrument parameters such as incidence angle, frequency and polarization (Hall, 1996). Microwave remote sensing measurements of bare soil surfaces are very sensitive to the water content in the surface layer due to the pronounced increase in the soil dielectric content with increasing water content (Ulaby *et al*., 1996). This is the fundamental reason why any microwave technique particularly in the low-frequency microwave region from 1–10 GHz, offers the opportunity to measure soil moisture in a relatively direct manner. For soil moisture retrieval studies, the most important bands are: L-band (frequency f= 1–2 GHz, wavelength h=30 – 15 cm), C-band (f= 4–8 GHz, h=7.5–3.8 cm) and X-band (f= 8–12 GHz, h= 3.8–2.5 cm) (Wagner *et al*., 2007). The retrieval of soil parameters from RADAR measurements have some problems, due to more than one combination of soil characteristics (in terms of SMC, roughness, vegetation coverage) leads to the same electromagnetic response at the sensor. Soil characteristics affect the microwave signal differently and to a different extent, depending on the sensor configuration (Paloscia *et al*., 2013). According to Paloscia *et al*. (2013), when dual-polarized (VV/VH or HH/HV) images are available, without NDVI ancillary information, the sensitivity of each polarization to the different surface features can be considered. This is used for distinguishing certain surface types and for evaluating the effect of the vegetation and soil conditions, in order to improve the accuracy of SMC retrieval. Recently, the soil moisture content retrieval algorithm from multi-temporal SAR data intended to use the Sentinel-1 Interferometric Wide Swath image data. The algorithm has been developed in the framework of the ESA project GMES (Global Monitoring for Environment and Security). According to Mattia (2011), Sentinel-1 soil moisture algorithm development was aimed at developing global near-real-time and off-line soil moisture content products at high spatial resolution. At microwave frequencies, the most striking feature of the emission from the earth's surface is a large contrast between water and land.

2.8 RADAR Polarization

Polarization refers to the spatial orientation of the plane of oscillation of the electric field that can be oriented vertically, horizontally or at some other angles. The possible combinations of polarization in microwave remote sensing includes vertical transmission and vertical reception (VV), horizontal transmission and horizontal reception (HH), horizontal transmission and vertical reception (HV) and vertical transmission and horizontal reception (VH) (Sarmap, 2009). Most remote sensing RADARs transmit linearly polarized signals. These are described as vertically (V) polarized if the electric field of the wave lies in the plane defined by the propagation direction and the direction of a line pointing outwards from the earth's center (a radius vector). Horizontally (H) polarized RADARs are formed when the electric field is perpendicular to this plane. The return signal typically contains both vertically and horizontally polarized components, which can be measured separately by an appropriately designed system. The measured signals are then described as the VV, VH, HV, or HH channels, where VH, for example, denotes V transmit, H receive.

2.9 Optical Remote sensing for Groundwater Zone Identification

Optical remote sensor images, particularly the multispectral optical images, are important for LU/LC mapping, which is one of the governing factors for identification of groundwater zones (Nizalapur, 2008). Optical remote sensing imageries are very important to map the surface morphological, hydrological and geological regime of a certain area, which primarily governs the subsurface water conditions (Meijerink, 2007).

2.10 Sentinel

The aim of the Sentinel mission is to support the Copernicus program, offering a significant scientific opportunity due to a broad variety of sensing methods, the compatibility with past ESA mission, and the distribution policy, which will guarantee free, full and open access to data (Amitrano *et al*, 2014). Therefore, the capacity of acquiring, interpreting and processing Sentinels' data will be crucial for the success of projects involving geographical information.

2.10.1 RADAR Sentinel family

The RADAR Sentinel-1 represents the new generation of the European Space Agency (ESA) in which, the main purpose is the monitoring of land and oceans while ensuring the continuity of SAR (C-band) data (ESA, 2014). Sentinel-1 is a two-SAR satellite constellation designed to guarantee global coverage with a revisit time of 6 days.

The first satellite (Sentinel-1A) was launched on 3 April 2014. Sentinel-1A is placed in a near-polar, sun-synchronous orbit with a 12-day repeat cycle and 175 orbits per cycle. Both the satellites of the Sentinel-1 constellation share the same orbit plane with a 180° orbital phasing difference (Donato *et al*., 2014). Sentinel-1 is designed to work with four different possible operative modes: (i) strip map, (ii) wave, (iii) interferometric wide swath and (iv) extra wide swath. Among these modes Interferometric Wide Swath (IW) is main operational mode on the Earth's surface) (Sentinel-1 User Handbook, 2013; ESA, 2014).

The identification of linear features is possible from RADAR image which expressed that the most of these features are perpendicular to sub-perpendicular to the look direction (strong return backscattering). Due to the higher sensitivity of RADAR to the surface geometry and surface roughness, extraction of geomorphology, geological structure, and lithology can be possible (Abuzied *et al*., 2016). According to Zakaria *et al*. (2017), lineament automatic extraction from optical remote sensing and RADAR sentinel family were extracted, and the result shows that Sentinel 1 data are more efficient in restitution of lineaments. This indicates the performance of the RADAR data compared to those optical data.

2.10.2 Optical Sentinel family

Sentinel-2 is a state of the art sensor launched on 23 June 2015 by the European Space Agency (ESA). The Sentinel-2 mission is a land monitoring constellation of two satellites that deliver high-resolution optical imagery and provide continuity for the existing SPOT and Landsat missions. It provides a global coverage of the Earth's land surface every 10 days with one satellite and every 5 days with the second satellite, making the data of great use in on-going studies (Addabbo *et al*., 2016). The system is designed to collect data at 10 m (blue, green, red and near-infrared-1) and 20 m (red edge 1 to 3, near-infrared-2, shortwave infrared 1 and 2). Three additional bands for atmospheric correction are collected at 60 m (for retrieval of aerosol, water vapor, cirrus), resulting in a total of 13 spectral bands (Ng *et al*., 217). The five to ten-day minimum revisit time of Sentinel-2 MSI is important for environmental and geological studies that require frequent data. Sentinel-2 is used for monitoring of geological activity associated with volcanoes, tectonics and geothermal systems as well as secondary effects related to earth sciences, such as land cover changes associated with natural degradation or natural hazards (Werff and Meer, 2016).

2.11 Groundwater in Ethiopia

The hydrological conditions which exist in the country are highly varied as a result of the complexity of geology, physiography and climate change. The aquifers are mostly in the moderate range of productivity and the depth to groundwater is generally less than 150 m (Tesfaye Chernet, 1993). According to Seifu Kebede (2010), the source of groundwater recharge in Ethiopia is under flood recharge, wadi flood recharge, rainfall recharge, mountain block recharge and runoff from graben. Tamiru Alemayehu (2006) investigated the occurrence of groundwater in Ethiopia and describe the most important factors governing the groundwater flow and storage in volcanic rocks. The variation in mineralogy, texture, and structure of volcanic rocks cause the variation of water-bearing capacity of the area. Groundwater is an important source of water and is the dominant source for domestic supply in many areas, especially the dry areas where surface waters are scarce and seasonal (British Geological Survey, 2001). In many parts of the country, groundwater is an important source of potable water. This is especially true for rural areas as well as for towns. According to Tesfaye Chernet (1993), The health of the population can be improved a great deal through an increased provision of clean and adequate water supplies mostly taken from groundwater. However, the occurrence of groundwater is not uniform due to various environmental and geological factors (Tamiru Alemayehu, 1993).

CHAPTER THREE

3 MATERIALS AND METHODS

3.1 Description of the Study Area

3.1.1 Location

The Ketar watershed is located in the central part of MER, which is a part of Arsi zone in Oromia region (Figure 3.1). The watershed is located in Ziway-Shala basin, which is 225 km far from Addis Ababa. The major towns in the area include Ogolcho, Gonde, Asela, Digelu, Sagure, Bekoji and Meraro. The watershed covers an area of 3354 km^2, which is bounded by longitudes 38° 52' 33"−39° 24' 36" E and latitudes 7° 21' 42"−8° 8' 5" N. Ketar river watershed area starts from the eastern Ethiopian plateau, south of Mararo town and ends at Lake Ziway in central part of MER floor, west of Ogolcho town. Ketar river is the main river in the watershed area.

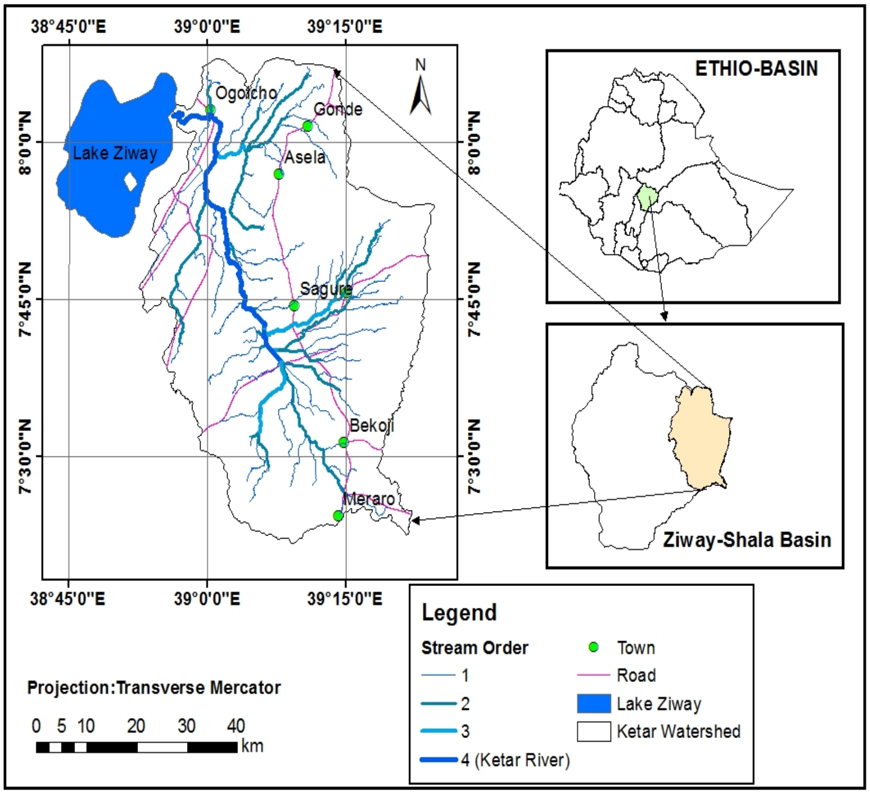

Figure 3.1: Location map of the study area

3.1.2 Socio-Economy of the study area

According to Ethiopian Central Statistical Agency (2007), the total population in the study area was 700,000. The average water conception is estimated 30 liters per inhabitant per day (Pascal-Ferrer and Candela, 2015). The major source of economic activity is agriculture. Population distribution and agriculture in highlands and lowlands have shown differences in properties due to rainfall variation. More rainfall in the highlands occur than in lowlands leads to two different agricultural systems in the two areas. In high land areas, most of the population use livestock as a source of income by grown animals for milk and meat production.

3.1.3 Topography and Drainage

The topography of the area is primarily determined by the rift system of faulting. Rift margin faults have undergone along a period of erosion while those of rift floor are mostly recent (Tesfaye Chernet, 1982). The rift floor consists mainly of extensive flat lands; while the escarpment areas have mostly steep slopes and cliffs. Ketar river watershed is bounded in the East, Southeast and South by a chain of mountains (Chilalo, Galama and kakka) while in the West and North- West bounded by Wonji fault belt produced horsts and volcanic cone formed from volcanic eruption following faulting. The altitude ranges from about 1628 to 4171 meters (Figure 3.2) above mean sea level (a.m.s.l). Katar river is the biggest perennial river starting around Kakka mountain and flows along the midline of the area towards the northwest where it joins Lake Ziway. The main perennial streams that feed river Ketar are Ashebeka, Worga, Tamela and Bosha. Small streams disappear in the rift before reaching the rift lakes by transmission losses in large faults and volcanic vent (Tenalem Ayenew, 1998). Ketar river and the upper said perennial as well as their intermittent tributaries, have given the area dendritic drainage pattern.

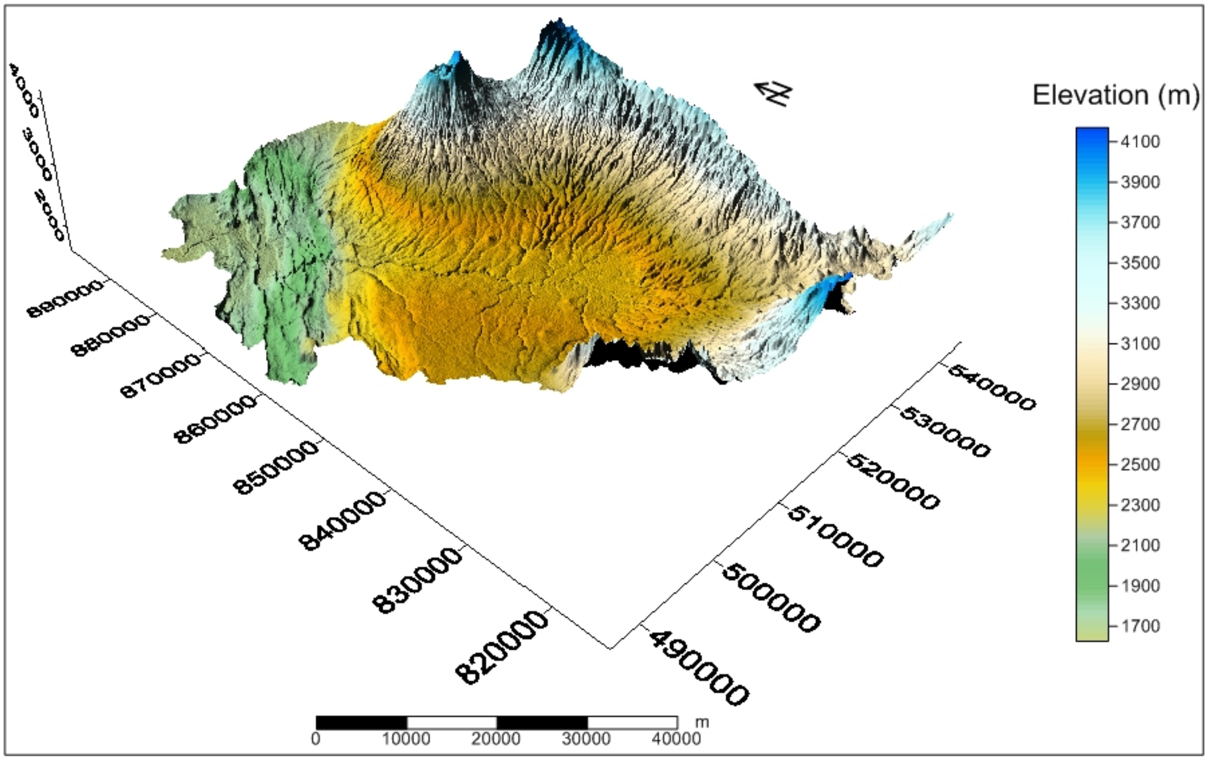

Figure 3.2: Physiographic map of the study area

3.1.4 Climate

In Ethiopia, most areas get the highest precipitation from rainfall of summer season June, July and August. According to Ethiopian National Metrological Agency (ENMA), the main form of precipitation is rainfall in the study area. For the most area of the Ketar watershed rainy season starts from March and extends to October with the highest rainfall concentration is in June, July, and August. The amount of rainfall varies from place to place in the watershed area. The mean annual rainfall for 30 years (1987–2016) over the watershed ranges from 740.2 mm at rift to 1,056.8 mm at highlands (Figure 3.3). This watershed is also characterized by high relief difference and ranges of temperature. The mean annual temperature in the study area varies from 6.52 in Meraro station to 27.75 of Ogolcho station (Figure 3.4).

Figure 3.3: Average annual rainfall (1987–2016)

Figure 3.4: Maximum and Minimum mean annual temperature of stations (1987–2016)

3.1.5 Geological units of the Study Area

According to Geological survey of Ethiopia studied by (Workineh Haro *et al*., 2014; Basalfew Zenebe *et al*., 2012 and Tsegaye Abebe, 2005) geological units in the watershed area (Figure 3.5) includes alluvial (Qa), basaltic hyaloclastics (phreatomagmatic deposits) (Qwh), Chefe Donsa Pyroclastic flows (Ncp), Pliocene trachyte (Tv7), Pliocene basalt flows (Tv6), high land basalt (Tv4), lacustrine sediments (Ql), Pleistocene basalt flows and cones (Qwbp), pumice and unwelded tuffs (Qwpu), recent and sub-resent basalt flows and cones (Qwbh) , rhyolitic and trachytic lava domes and flows (Qwa), ignimbrites, tuff and waterlain pyroclastics (Qdi) and

upper pyroclast (Tv3), which contains mainly layers of massive to welded ignimbrite, loose volcanic ash, tuff and lapilli tuff. The detail description of each geological unit is illustrated in (Appendix II).

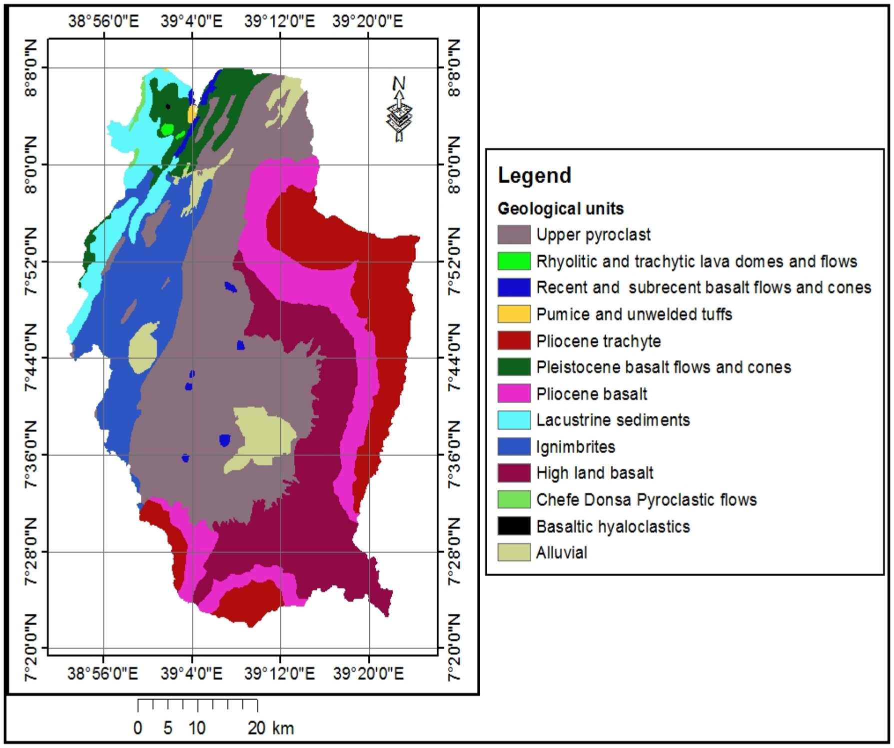

Figure 3.5: Geological unit map of the study area modified from: Workineh Haro *et al*, 2014; Basalfew Zenebe *et al*, 2012 and Tsegaye Abebe, 2005

3.1.6 Soil

The soil type in the study area contains four soil texture categories namely clay, loam, loamy sand and sandy loam (Figure 3.6). Most of the watershed area covers by clay and loam soils (Table 3.1). Sandy soils are derived from ignimbrites, unwelded pumiceous pyroclastics and some coarse beds of lacustrine sediments (Tesfaye Chernet, 1982).

Table 3.1: Soil texture and study area coverage

Soil texture type	Area coverage (km^2)

Clay	1715.70
Loam	1587.67
Sandy Loam	49.01
Loamy Sand	1.62

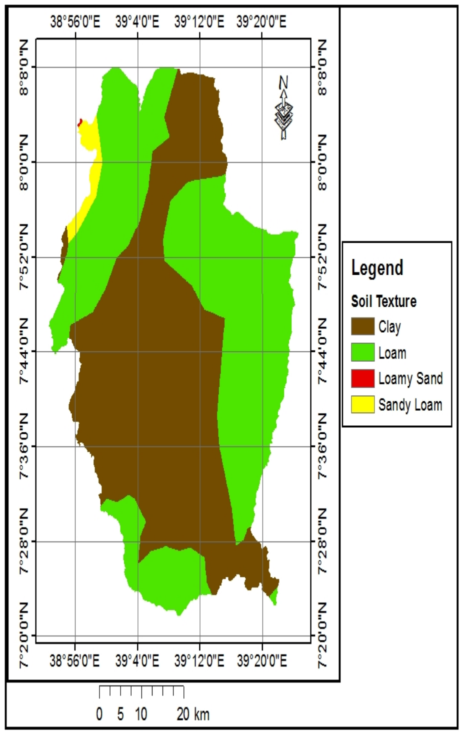

Figure 3.6: Soil texture map of the study area (OWWDSE, 2017)

3.2 Data Description and Material Used

3.2.1 Data Description

The primary and secondary data that were identified as parameter factors for analysis were collected from different sources (Table 3.2). The primary data includes cloud free sentinel-2A image (spatial resolution of 10 m), RADAR sentinel-1A and DEM (10 m × 10 m) which was derived from RADAR sentinel-1A image. The secondary data were used from published and unpublished documents from different organizations. Geology and demographic characteristics data were gathered from Geological Survey and Central Statistical Agency of Ethiopia, respectively. Climatic data were collected from Ethiopian National Meteorological Agency (ENMA), which includes mean annual precipitation and temperature for all 8 metrological stations belongs to the study area for 30 years records (1987−2016). Soil type in texture data was collected from Oromia Water Works Design and Supervision Enterprise.

Table 3.2: Geospatial data used in this research

Dataset	Source	Output Layer
Sentinel-1A (10 m)	Copernicus hub (https://scihub.copernicus.eu)	Lineament density and Soil moisture
Sentinel-2A (10 m)	Copernicus hub (https://scihub.copernicus.eu)	LU/LC
DEM (10 m)	Sentinel-1A	Slope, drainage density, lineament density, geomorphology
Rainfall	Ethiopian National Metrological Agency	Mean annual rainfall
Soil	Oromia Water Works Design and Supervision Enterprise	Soil texture
Geology	Ethiopian Geological Survey	Geological units of the study area

3.2.1.1 Sentinel-1A Synthetic Aperture Radar (SAR)

The Sentinel-1 is an active RADAR imaging satellite which delivers images both at day and night under all weather conditions. The mission of Sentinel-1 is the European Radar Observatory for the Copernicus combined initiative of the European Commission (EC) and European Space Agency (ESA). The mission includes C-band SAR instrument, which is composed by a constellation of 2 polar-orbiting satellites, Sentinel-1A and Sentinel-1B, sharing the same orbital plane. Sentinel-1 potentially operates in four acquisition modes: Interferometric Wide swath (IW), Strip map (SM), Extra-Wide swath (EW) and Wave (WV). Most remote sensing RADARs transmit linearly polarized signals. These are described as vertically (V) polarized when the electric field of the wave lies in the plane defined by the propagation direction and the direction of a line pointing outwards from the earth's center (a radius vector), and as horizontally (H) polarized when the electric field is perpendicular to this plane. The return signal typically contains both vertically and horizontally polarized components, which can be measured separately by an appropriately designed system. The measured signals are then described as the VV, VH, HV, or HH channels. SAR instrument can operate in single polarization (HH or VV) and dual polarization (HH+HV or VV+VH), through one transmit chain (switchable to H or V) and two parallel receive chains for H and V polarization. SM, IW, and EW are available in single (HH or VV) or dual polarization (HH+HV or VV+VH). Wave is single polarization only (Sentinel-1User Handbook, 2013).

Sentinel-1A SAR image (GRD product, VH polarization, IW mode) of an acquired date on January 4, 2017, was downloaded for this study from the European Space Agency (ESA) through the Sentinels scientific data access available on the Copernicus scientific data hub.

3.2.1.2 Sentinel-2A Multi-Spectral Instrument (MSI)

Sentinel-2A is a key element of the Copernicus program of the European Union and features a two-satellite land monitoring constellation designed by the European Space Agency (ESA) and built by Airbus Defense and Space. Sentinel 2's instruments comprise 13 spectral channels with a 290 km swath and spatial resolutions of 10 m (4 visible and near-infrared bands), 20 m (6 red-edge/shortwave infrared bands) and 60 m (3 atmospheric correction bands). It is able to support a wide range of land studies and geophysical applications, reducing the time required to build a rich and worldwide cloud-free imaging archive. The spectral bands of Sentinel-2 provide data for land cover and change classification (http://www.copernicus.eu). A Sentinel-2 image is a compilation of granules of fixed length (approximately 25 km across the track and 23 km along the track) and area (100 km^2 in UTM/WGS84 projection) available to the user in SENTINEL-SAFE format (https://sentinel.esa.int/web/sentinel/user-guides/sentinel-2-msi/data-formats). For this study, the selected bands of Sentinel-2 for stacking were bands of (2, 3, 4, 8, 11 and 12) which are corresponding to Landsat bands of (blue, green, red, near-infrared, shortwave infrared1 and shortwave infrared 2) results in a product close to TM / ETM+ / OLI.

3.2.2 Material Used

In order to achieve the objectives of this study, the following hardware and software were utilized:

Hardware used

External Hard disk: 1 TB storage size.

Handheld GPS receiver: Garmin 78, with 3 m positional accuracy was used for sample point collection for LU/LC verification.

Laptop with a monitor display of 1366x768 pixels, Memory, 4.0 GB RAM and 2.7 GHz processor speed was used.

Software used

The different software that was used for this study includes;

ArcGIS 10.3: ArcGIS 10.3 was used for RADAR image processing (to convert the row image into decibel value), storing and managing geographic data in geodatabase package, compile and edit GIS datasets and display and analyze spatial data in both vector and raster format and finally to prepare each thematic layer.

ERDAS Imagine 2015: This was used for mosaicking, classification and post-classification of the Sentinel-2A image for LU/LC preparation.

SNAP: This software was used for pre-processing of the Sentinel-1A image.

IMPACT-Toolbox: IMPACT-Toolbox software was used for atmospheric correction and layer stacking of sentinel-2A images.

IDRISI Selva 17.00: Idrisi Selva was used for aggregation of reclassified factors based on AHP criterion weight.

Surfer 10: This software was used for physiographic map preparation.

3.3 Methods

The following methodological approach was employed in carrying out this research.

1. Thematic layer preparation: Appropriate layers were prepared using sentinel family Satellite data, DEM and other thematic and collateral data.

2. Data analysis and integration: Digitization, data editing, field verification, data validation, data integration, attribute table design and entry were done based on the layers prepared in stage 1.

3. Developing Decision Rule: The following consecutive procedures were undertaken to come out successful results. These were standardizing criteria, reclassifying input layers, multicriteria and AHP analysis, criterion weight, weighted linear combination, identifying potential groundwater zones and validation of potential groundwater zone.

3.3.1 Parameter Identification for Groundwater Zones

Parameters influencing the occurrence of groundwater potential zones were identified from different previous kinds of literature. Those parameters which have a significant role in the identification of groundwater potential includes geological unit, rainfall, soil texture, geomorphology, slope, drainage density, lineament density, soil moisture and LU/LC. Overview of the methodology is illustrated in the following methodological flow chart (Figure 3.7).

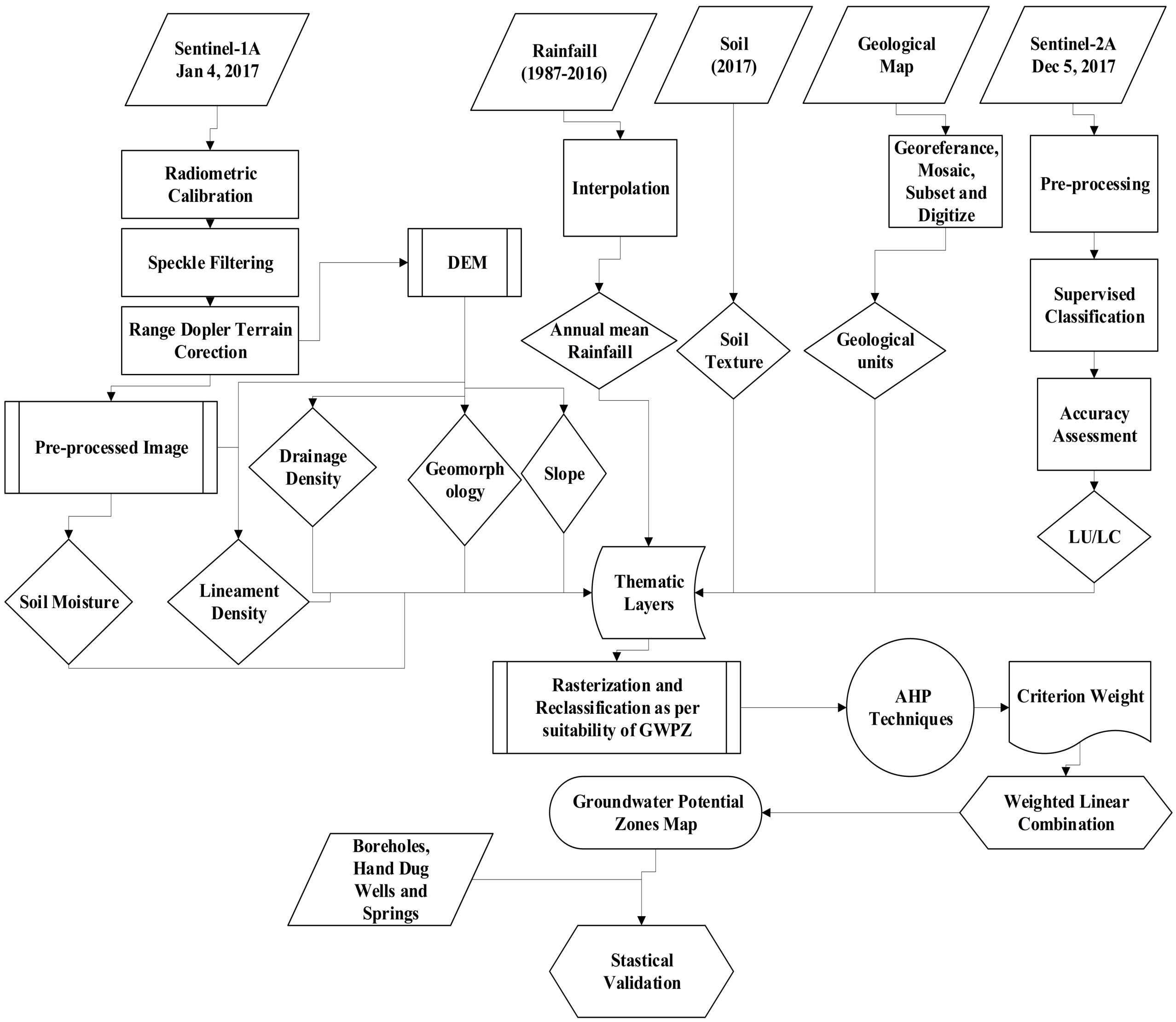
Sentinel-1A
Jan 4, 2017
Rainfaill
(1987-2016)
Soil
(2017)
Geological
Map
Sentinel-2A
Dec 5, 2017
Radiometric
Calibration
Interpolation
Georeferance,
Mosaic,
Subset and
Digitize
Pre-processing
Speckle Filtering
DEM
Range Dopler Terrain
Corection
Annual mean
Rainfaill
Soil
Texture
Geological
units
Supervised
Classification
Accuracy
Assessment
Pre-processed Image
Drainage
Density
Geomorph
ology
Slope
LU/LC
Soil Moisture
Lineament
Density
Thematic
Layers
Rasterization and
Reclassification as per
suitability of GWPZ
AHP
Techniques
Criterion Weight
Groundwater Potential
Zones Map
Weighted Linear
Combination
Boreholes,
Hand Dug
Wells and
Springs
Stastical
Validation

Figure 3.7: Methodological flow chart of the study

3.4 Data Analysis

In this section the procedure for identification of relevant evaluation criteria data sets through data collection, data preparation/organization, data pre-processing and editing, analysis, field verification, data validation, data Integration, attribute table design and entry, standardizing criteria and overlay technique was covered.

3.4.1 Pre-processing

Pre-processing was done on the raw data of the two sentinel family images (sentinel-1A and sentinel-2A). The pre-processing which was done on these data include the radiometric and geometric correction.

3.4.1.1 Sentinel-1A Pre-processing

The main pre-processed stages that were used for this study includes image calibration, speckle filtering, and geometric terrain correction.

Image Calibration

Typical SAR data processing, which produces level 1 image, does not include radiometric corrections and significant radiometric bias remains. Therefore, it is necessary to apply the radiometric correction to SAR images so that the pixel values of the SAR images truly represent the RADAR backscatter of the reflecting surface. Image calibration was performed as one of the SAR image preprocessing steps using sentinel application platform (SNAP). The objective of SAR calibration is to provide imagery in which the pixel values can be directly related to the RADAR backscatter measured in decibel (dB) of the scene (Getu Tesema, 2017). According to Martinis and Rieke (2015), the data calibration compensates for the radiometric influences of different incidence angles- caused by the sensor geometry and topographic characteristics of the surface. For converting digital pixel values to radiometrically calibrated backscatter, all the required information found in the product metadata. In this study, Sentinel 1A image was used, at L1 GRD (Ground Range Detection) level and IW mode with the polarizations (VH). These are Digital Number (DN) data that require conversion to backscatter values reflected by the surface. The RADAR cross-section sigma naught (σ^0) was used as sentinel-1 data calibration product. It was possible to calibrate the sentinel-1 GRD product using SNAP toolbox automatically by equation (1).

(1)

Where; : is the pixel digital Number of GRD pixel amplitude, directly taken from the measurement file and A is the value of sigma () in the product metadata. The backscattering coefficient is expressed in decibels using equation (2) (Navarro *et al*, 2016):

(2)

Speckle Filtering

Synthetic Aperture Radar images have inherent salt and pepper like texturing called speckles which degrade the quality of the image and make interpretation of features more difficult. Speckles are caused by random constructive and destructive interference of the de-phased but coherent return waves scattered by the elementary scatters within each resolution cell. Speckle noise reduction can be applied either by spatial filtering or multi-look processing. Speckle is a signal-dependent noise which is natural to any images obtained by coherent radiation, including SAR. Unlike optical remote sensing images which are characterized by very neat and uniform features, SAR images are affected by speckle (Babu *et al*., 2013). The speckle filtering carried out in this study was single product speckle filter type focused on the single date SAR image filter using Lee Sigma filtering type with the same window kernel size (7×7) which is the optimal SAR filtering kernel (Table 3.3).

Table 3.3: Speckle Filtering

Single product speckle filter	
Source Band	Amplitude VH
Filter	Lee sigma
Number of looks	1
Window size	7×7
Sigma	0.9
Target window size	3×3

Range-Doppler Terrain Correction

Due to topographical variations of a scene and the tilt of the satellite sensor, distances can be distorted in the SAR images. Image data not directly at the sensor's nadir location will have some distortion. Terrain corrections are intended to compensate for these distortions so that the geometric representation of the image will be as close as possible to the real world. The Range Doppler Terrain Correction Operator implements the Range-Doppler orthorectification method for geocoding SAR images from single 2D raster RADAR geometry (Small and Schubert, 2008). The Range Doppler Orthorectification method was used to geolocate all the SAR images using available orbit state vector information in the metadata, the RADAR timing annotations, the slant to ground range conversion parameters together with the reference DEM data. The DEMs with geographic coordinates with points of latitude, longitude, and height (P_{lat}, P_{lon}, P_h) referred to global geodetic ellipsoid reference WGS84 and height in meters are properly supported. For this study, using sentinel-1A SAR image, different processing parameters (Table 3.4) have used for Range Doppler Terrain Correction and automatic DEM extraction. The backscattered value is different from place to place. This is because when microwaves strike a surface, the amount of energy scattered back to the sensor depends on various factors like geometric factors (surface roughness, slopes, orientation of the objects), physical factors of surface material (moisture content), the types of land-cover (soil, vegetation or man-made objects) and microwave frequency, polarization and incident angle. The value of the processed image is expressed in decibel (dB) which shows the backscattered value. Areas which have more dB value is due to double bounce of microwave energy.

Table 3.4: Range Doppler Terrain Correction method

	Processing parameter
Source band	Amplitude VH
DEM resampling method	Bilinear interpolation
Image resampling method	Bilinear interpolation
Pixel spacing in (m)	10
Map projection	UTM Zone 37 WGS 1984

Digital Elevation Model Extraction from Sentinel-1A

Digital Elevation Models that are used for visualizing the earth are growing with update technology. Radar technology and connected technologies like SAR and InSAR, grow up day by day fast (Makineci and Karabork, 2016). For this study, DEM image was automatically generated while terrain correction from the Sentinel-1A SAR image. Digital Elevation Model (Auto download) with bilinear interpolation method was used to derive. The DEM image has the same dimension as the processed SAR image. The pixel value of the DEM image is the elevation of the corresponding pixel in the SAR image.

3.4.1.2 Sentinel-2A Pre-processing

Sentinel-2 data are acquired on 13 spectral bands in the VNIR and SWIR, which have different spatial resolutions (10 m, 20 m and 60 m). Due to this, it is necessary to set a common output projection and resolution using IMPACT-Toolbox software. Considering this, nearest neighbor resampling was used for this study while staking together bands of different resolution to get highest resolution image (10 m). Radiometric resolution of sentinel-2 MSI is 12 bit, saved using Unsigned integer 16-bit data type. By selecting Byte, output radiometric resolution has converted into Byte by using a linear transformation Top of Atmospheric Reflectance Byte (TOARB) using equation (3).

$$TOARB = (DN*0.0255) \quad (3)$$

Image DN values [0-4095] were converted to TOA Reflectance [0,1] using the provided conversion factor (10000) and multiplied by 255 to obtain a byte TOA Reflectance [0,255] (https://sentinel.esa.int/web/sentinel/user-guides/sentinel-2-msi/resolutions/radiometric).

3.4.2 Criteria Thematic Layer Preparation

Thematic layers were prepared by assigning different criteria for each layer as per suitability of groundwater potential zones. Criteria for those layers were given using different previous kinds of literature. The criterion of thematic layers was converted into raster data format using one of the required attributed columns to form each layer. All converted layers were reclassified according to reviewed literature and some of them were customized in order to meet the site-specific requirement. All criteria for thematic layers have the same cell size. Resampling technique was used for cell size similarity of 10 m. The reclassification was used to simplify the interpretation of raster data by changing a single input value into a new output value. It also used to group ranges of cell values into a single value. By using reclassified layers, which results in a generalization and simplification of the original dataset, input layers were categorized based on the same ranking scheme that can be used to compare and rank the least and most suitable sites. For this study, after all sinks and cuts were filled in order to keep continuity of flow to the watershed of study area; slope, geomorphology, and hydrological parameters such as flow direction, flow accumulation, stream network, stream order and drainage density were derived from the DEM of 10 m resolution (DEM from sentinel-1A image). Lineament density was prepared from sentinel-1A and DEM. Soil moisture zones were derived from sentinel-1A pre-processed image. Land-use/land-cover was prepared from sentinel-2A processed image. Other layers like rainfall, soil texture and geology were prepared as per suitability for potential groundwater zones.

3.4.2.1 Slope

The slope is one of the important terrain parameters which are explained by the horizontal spacing of the contours. In general, in the vector form closely spaced contours represent steeper slopes and sparse contours exhibit gentle slope whereas in the elevation output raster every cell has a slope value. Here, the lower slope values indicate the flatter terrain (gentle slope) and higher slope values correspond to the steeper slope of the terrain. In the elevation raster, the slope is measured by the identification of maximum rate of change in value from each cell to neighboring cells (Waikar and Nilawar, 2014). The slope is one of the most significant parameters for groundwater exploration. The slope of any area affects the runoff and recharge of surface water. In terms of groundwater recharge, an area with flat terrain topography falls into the very good category and has relatively more infiltration rate (Barik *et al*., 2017). This is because increased slope results in high runoff and erosion of surface soil (Ibrahim-Bathis and Ahmed, 2016). Gentle and nearly level surface slope allows water to flow very slowly and have enough time to infiltrate into the soil. The slope in the study area ranges from 0 to 58 degrees (Figure 3.8). As per suitability for identification of potential groundwater zones, the slope in the study area was reclassified into five (Table 3.5).

Table 3.5: Slope suitability for identification of groundwater potential zones

Slope in degree	Slope category	Ranking	Classification
>30	Very steep	1	Very poor
10–30	Steep	2	Poor

5–10	Moderate	3	Moderate
2–5	Gentle	4	Good
0–2	Level	5	Very good

Source: (Rather and Andrabi, 2012)

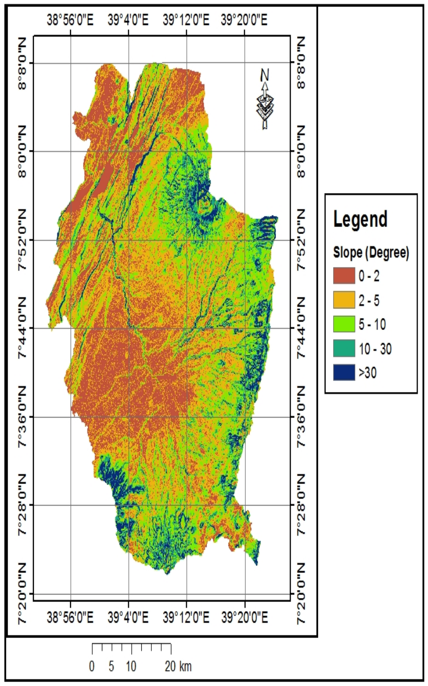

Figure 3.8: Slope map of the study area

3.4.2.2 Drainage Density

Drainage density was defined by Horton (1945) as the ratio of the total length of streams in a watershed over its contributing area as stated in equation 3. In this study, the hydro-processing tool was used for extraction of drainage from DEM of Sentinel-1A.

(3)

Where = Drainage density, = = Total length of all stream segments in a given basin and = Total area of the watershed area. In the present study, the following hydrological parameters were extracted from hydrological tools of ArcGIS environment to prepare layers for drainage density. The methods followed to calculate the drainage density and stream order calculation was done as shown below.

Flow Direction

The flow direction of the study area was calculated using flow direction tool, which creates a raster of flow direction from each cell to its steepest downslope neighbor, by computing the flow direction for a given grid. The value in any given cell of the flow direction grid indicates the direction of the steepest descent from that cell to one of its neighboring cells using the eight directions (Getachew Haile, 2017). This operation was used for required input to create stream order raster for the next steps of drainage creation and as input for flow accumulation calculation.

Flow Accumulation

The flow accumulation raster layer was derived from flow direction raster grid as input, in order to determine the accumulated number of raster grids that are draining to each raster grid on the surface. The result of this function was a raster of accumulated flow to each grid, as determined by accumulating the weight for all grids that flow into each downslope grid. This was used to generate stream, which is required as an input to create stream order of the watershed.

Stream Raster

The detail steams of the area were calculated and derived from flow accumulation that gives the number of raster grid cells that drain to a particular grid cell, which was used to define a stream. A stream is formed when a certain threshold area drains to a point. This threshold is defined by using the amount of raster grid cells in the flow accumulation grid. For this study, thirty thousand threshold values were used to form a stream raster. Grid cells that have more than 30,000 cells flowing into them were used to define the stream network. Con tool was used in ArcGIS software environment to create a stream network raster where flow accumulation values of 30,000 or greater go to one, and the remained are put to the background (No Data).

Strahler Stream Order

Stream order (Figure 3.9), which is used as an input for generation of drainage density was derived from stream raster of the area. A headwater stream with no tributaries is considered as a first-order stream. A segment downstream of the confluence of two first order streams is a second order stream (Strahler, 1952). Thus, n^{th} order stream is always located downstream of the confluence of two n-1th order streams. Stream order only increases when streams of the same order intersect. In groundwater potentiality, the highest the stream order has the highest occurrence of groundwater and the smallest steam order has the smallest occurrence of groundwater (Rather and Andrabi, 2012). Most of the drainages in the study area flow from Southeast high land area to North West direction and form the main river called the Ketar.

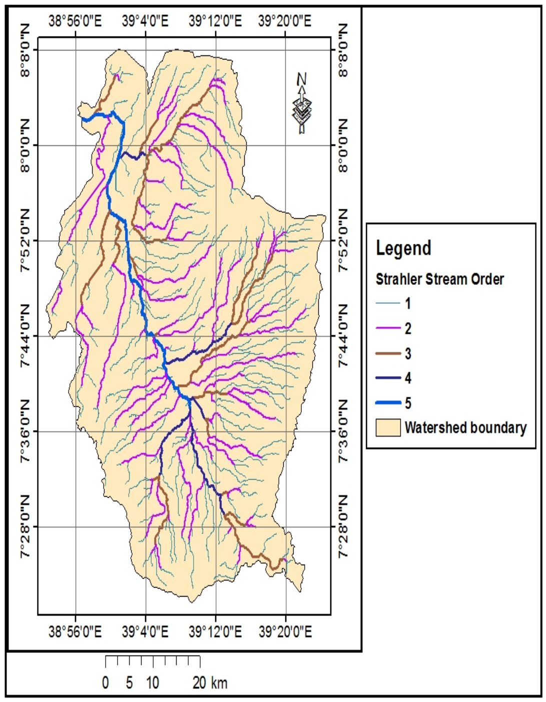

Figure 3.9: Stream Order map of the study area

The drainage density of the study area ranges from 0 to 4.2 km/km^2 (Figure 3.10). Areas of high drainage density have high runoff and less infiltration results in less occurrence of groundwater and the reverse are true, low drainage density has less runoff as well as has enough time to infiltrate to the ground results for the high occurrence of groundwater (Waikar and Nilawar, 2014). The drainage density in the study area was reclassified into five classes as per suitability rank of potential groundwater zone identification. As drainage density increases the potentiality to occur groundwater decreases (Table 3.6).

Table 3.6: Drainage density suitability for identification of groundwater potential zones

Drainage density (km/km^2)	Description	Ranking	Classification
0–0.5	Very low density	5	Very good
0.5–1.2	Low density	4	Good
1.2–2.4	Moderate density	3	Moderate
2.4–3.6	High density	2	Poor
3.6–4.2	Very high density	1	Very poor

Source: (Waikar and Nilawar, 2014)

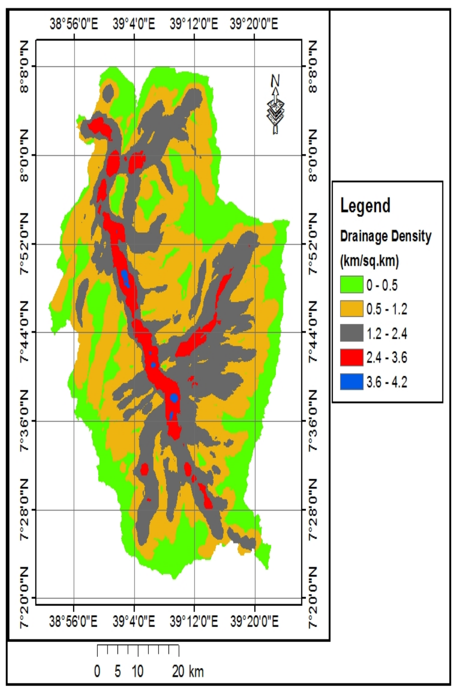

Figure 3.10: Drainage density map of the study area

3.4.2.3 Geological units

Geological units are major factors controlling the quantity and quality of groundwater occurrence in a given area. It is represented by the distribution of different rock units characterizing the area under study (Mwega *et al*., 2013). According to Mwega *et al*. (2013), Sedimentary rocks were considered as having a high potential for groundwater due to their high porosity and permeability relative to other rocks. Classification of lithostratigraphic units into hydrostratigraphic units requires information on the hydraulic characteristics of rocks (Tenalem Ayenew, 1998). Large spatial variation in the permeability of rocks is a common feature of fractured volcanic terrain due to differences in the degree of fracturing. According to Tesfaye Chernet (1982), variable groundwater potentials are observed in the study area. Some massive pumiceous pyroclastics have poor yields while well jointed or fractured ignimbrites have good yields.

Groundwater Aquifer Characteristics

According to Tesfaye Chernet (1982), the different rock types mentioned on geological units of the study area are put into five groups based on hydrological characteristics.

1: Alkaline basalts, trachytes and trachybasalts

The mountains of eastern highlands of Chilalo, Badda, Kakka, and Kubsa are made up of these formations. These rocks have a variable degree of jointing and often they are massive to moderately jointed. Springs discharge at contacts of jointed and massive flows. Some of these springs are starting points for perennial streams which flow down to the lakes.

2: Ignimbrites and tuffs

They are the most extensive unit covering the rift floor and it is best observed at fault scraps. They are mostly well jointed and have a high or moderate permeability. However, when they are pumiceous or massive they have low permeability. Their thickness is mostly greater than 200 m.

The dense wonji fault belt cuts such rocks and increases the degree of jointing of the rock and increases the permeability

3: Recent basalts

These basalt flows have up to 100 meters thick occur east of Lake Ziway in the study area. The recent basalts have moderate to high permeability.

4: Pumice falls and acidic volcanics

They occur partly in mountains north of Lake Ziway. The pumice fails are characterized by a high inter-granular permeability which becomes highest when sorted. The acidic volcanics show moderate to high jointing.

5: Lacustrine sediments

They form the second largest outcrop next to the rift floor ignimbrites and they overlay the ignimbrites. They consist of alternating fine and course beds. The permeability of the lake sediment becomes higher when there is a higher proportion of coarser material like pumice sand beds. The thickness of the lake sediments ranges from 40 meters to more than 200 meters and on average they are 40-50 meters thick.

In the study area, the fractured and jointed ignimbrite and basalts are Permeable and facilitate the infiltration amount and rate (Astatke Kiflu *et al*., 2002). Therefore, the major potential rock units for the storage and movement of ground water in the study area are fractured volcanic rocks. The highlands of the study area (mountain Chilalo, Badda, Kaka and Kubsa) are characterized by less fracturing and weathering effect to depth. Geological units in the watershed area were illustrated in (Table 3.7) and reclassified into five based on permeability and degree of fracturing.

Table 3.7: Geological units suitability for identification of groundwater potential zones

Types of Geological unit	Rank in number	Classification
Upper pyroclast (loose volcanic ash, tuff and lapilli tuff), Pliocene trachyte and Pliocene basalt	1	Very poor
Pumice and unwelded tuffs	2	Poor
Chefe Donsa pyroclastic flows, rhyolitic and trachytic lava domes and flows, high land basalt	3	Moderate

Lacustrine sediment and alluvial	4	Good
Ignimbrites, recent and sub-recent basalts, Pleistocene basalt and basaltic hyaloclastics	5	Very good

3.4.2.4 Soil Texture

The texture is an estimate of the amounts of sand, silt, and clay in a soil. The mineral part of soil is a result of the breakdown of rock into sand and silt, and the recombining of some minerals to form clay. Soil texture consistently controls the penetration of surface water into an aquifer system (Oh *et al*., 2011). According to Fashae *et al*. (2014), the rate of infiltration largely depends on the grain size and related hydraulic characteristics of the soils. Different soil types have a different rate of infiltration, which results in different groundwater potential zones (Table 3.8). Fine-grained soils limit infiltration due to apparently low permeability, unlike coarse-grained soil materials where water can infiltrate easily because of high permeability (Fashae *et al*, 2014). The soil type in the study area contains four soil texture categories namely clay, loam, loamy sand and sandy loam. When a texture class is given a name, the dominant soil particle or its major texture class comes last. A sandy loam soil is a loam with a high sand content. A loamy sand is a sand which is approaching the texture of a loam, but it feels more like a sand than a sandy loam. Sands are dominated by sand particles, and therefore are the coarsest soils. Loams have a fairly mix of sand, silt and clay. When there is plenty of organic matter present in the loamy soil, their feel can be described as smooth or silky, and also greasy. Clay soils are referred to as fine-textured or heavy soils. Clay soils have a plastic feel when molded. The soil types in the study area are reclassified as per suitability for potential groundwater zones.

Table 3.8: Soil texture suitability for identification of groundwater potential zones.

Factor	Type in texture	Rank	Classification
Soil Texture	Clay	1	Very poor
	Loam	3	Moderate
	Sandy Loam	4	Good
	Loamy Sand	5	Very good

Source: (Ibrahim-Bathis and Ahmed, 2016)

3.4.2.5 Rainfall

Intensity and duration of rainfall play a significant role in infiltration. High intensity and short duration rain possess less infiltration and more surface runoff. Low intensity and long duration rain possess high infiltration than the runoff (Ibrahim-Bathis and Ahmed, 2016). Rainfall in the precipitation pattern may be influenced by the irregular topography. The large variability in altitude, slope, and aspect may increase variability by means of processes such as rain shading and strong winds (Tao *et al*., 2009). Accurate estimation of the spatial distribution of rainfall and extrapolation of point measurements over large areas is complicated. The best method to improve the quality of spatial rainfall estimation is to increase the density of the monitoring network. Rainfall can be interpolated using averaged values ranging from daily, monthly or annual aggregation levels, using a number of modern interpolation methods. For this study, eight rain gage stations were used for rainfall interpolation using deterministic and geostatic methods of IDW and kriging respectively. Based on root mean square error (RMSE) of IDW and ordinary kriging results, IDW was selected for interpolating the precipitation data for the entire study area. This is because interpolated rainfall results from IDW has less RMSE than ordinary kriging. IDW algorithm estimates cell values by averaging the values of nearby sample data points. From the interpolated result, maximum rainfall was recorded around Assela and Bekoji areas. Minimum rainfall was recorded around Sagure and rift floor part of the study area. High rainfall area has a high probability of recharge relatively too low rainfall area (Mwega *et al*., 2013). The mean annual rainfall ranges from 740.2 to 1,056.8 mm (Figure 3.11) and reclassified into five classes based on suitability rank of groundwater occurrence (Table 3.9).

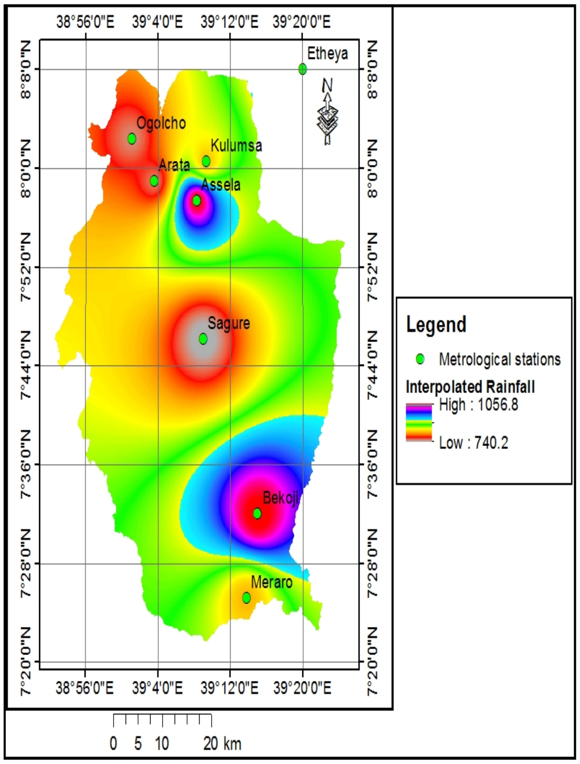

Figure 3.11: Mean annual rainfall of the study area (1987–2016)

Table 3.9: Rainfall suitability for identification of groundwater potential zones

Factor	Class	Rank	Classification
Rainfall (mm)	740.2–809.7	1	Very poor
	809.7–859.4	2	Poor
	859.4–909.0	3	Moderate
	909.0–971.1	4	Good
	971.1–1,056.8	5	Very good

3.4.2.6 Lineament Density

Lineaments are the linear, rectilinear and curvilinear features of tectonic origin observed on the satellite image. These lineaments normally show tonal, textural, soil tonal, relief, drainage and vegetation linearities and curvilinearities on satellite data (Sivakumar, 2015). According to Jhariya *et al.* (2016), lineaments can be mapped with the help of satellite data which are correlated with faults, fractures, joints, bedding planes and geological contacts which are useful for the groundwater potential study. The ability to identify lineaments on satellite image depends on the spatial resolution of the image (Alonso-Contes, 2011). Due to its high resolution, lineaments for this study were extracted from processed SAR and DEM of Sentinel-1A image,

(Figure 3.12a). Short lineaments were identified easily from Sentinel-1A SAR image. In the study area, most of the lineaments are aligned NE-SW direction like MER. The lineament map is then converted into zones of different lineament density. Lineament density is defined as the total length of all the lineaments demarcated divided by the total study area expressed in (Km/Km^2). In the study area, most lineament densities are found in North West part of the study area (Figure 3.12b). The lineament density in the study area ranges from 0 to 1.4 km/km^2. Lineament density for groundwater exploration was important because the joints and fractures serve as conduits for movement of groundwater and have a high water-holding capacity (Preeja *et al*., 2011). Hence, the high weight value for a groundwater potential area is high lineament density area (Das, 2017). The lineament density was reclassified into five as per suitability rank of groundwater occurrence (Table 3.10).

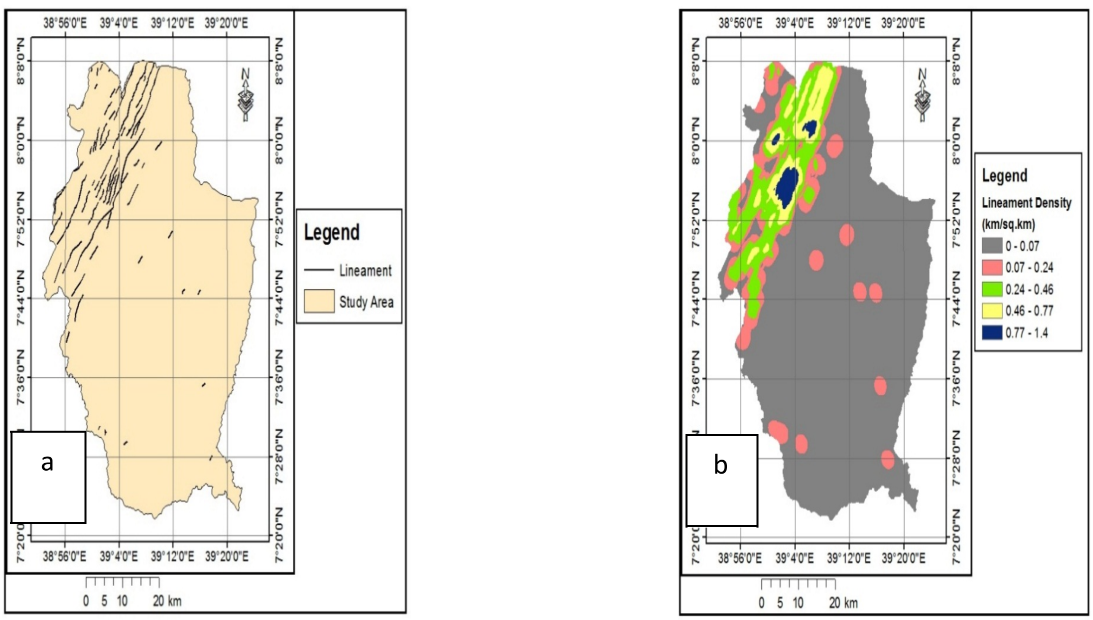

Figure 3.12: Lineament map (a) and Lineament density map (b) of the study area

Table 3.10: Lineament density suitability for identification of groundwater potential zones

Factor	Density (km/km^2)	Rank	Classification
Lineament density	0–0.07	1	Very poor
	0.07–0.24	2	Poor
	0.24–0.46	3	Moderate
	0.46–0.77	4	Good
	0.77–1.4	5	Very good

3.4.2.7 Land-use/Land-cover

Land-use/Land-cover plays a vital role in groundwater searching. Land-use type gives the necessary information on infiltration. The rate of recharge, runoff and evapotranspiration are influenced by the type of LU/LC. Land-use/Land-cover of the study area was prepared from sentinel-2A using maximum likelihood classification technique with the integration of field and google earth verification. The type of LU/LC includes farmland, shrubland, grassland, bareland, forest, settlement, wetland and waterbody (Figure 3.13). Validating LU/LC products provides critical data quality information to users and producers of these maps. A common practice is to conduct an accuracy assessment of the classified map based on a spatially explicit comparison of the map to a higher-quality reference data (Stehman and Wickham, 2011). The classification accuracy of this study was done based on field and Google earth reference data. The total reference data were 275, and the overall classification accuracy was 85.45% (Annex V). From the total study area, farmland covers most of the area and water body covers small area relative to others (Table 3.11).

Table 3.11: Land-use/Land-cover types and coverage of the study area

LU/LC	Area (km^2)	Area (%)
Farmland	2242.58	66.86
Shrubland	354.26	10.56
Bare-land	312.21	9.31
Grassland	300.69	8.97
Forest	109.08	3.25
Settlement	15.62	0.47
Wetland	15.95	0.48
Waterbody	3.61	0.1
Total	3354	100

The occurrence of groundwater is affected by the type of LU/LC. Considering this, LU/LC of the study area reclassified into five (Table 3.12) as per suitability rank of recharge information.

Table 3.12: Land-use/Land-cover suitability for identification of groundwater potential zones

Factor	Type	Rank	Classification
LU/LC	Bare-land and Settlement	1	Very poor
	Shrubland	2	Poor
	Farmland and Grassland	3	Moderate
	Forest	4	Good
	Waterbody and Wetland	5	Very good

Source: (Das, 2017)

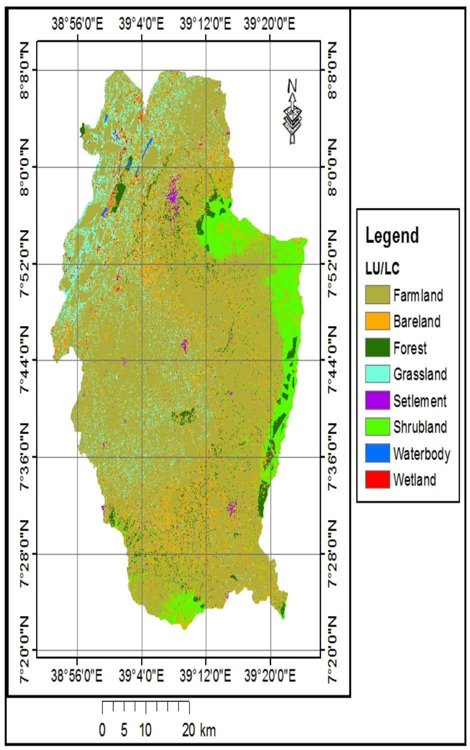

Figure 3.13: Land-use/Land-cover map of the study area

3.4.2.8 Geomorphology

Physiographical analysis of an area has a vital role in groundwater exploration (Rather and Andrabi, 2012). The volcanic terrain of Ethiopia comes in a variety of landforms that has a significant importance to groundwater occurrence and movement (Von and Seifu Kebede, 2012). The identification of landforms and geomorphological domain by using remotely sensed data is based on area association (arid, mountainous, glacial, coastal, floodplain, tropical etc.), association of features, landform shape and size, drainage patterns, relief, tone, texture, LU/LC, erosion and other patterns (Lwin and Khaing, 2012). Digital elevation models (DEMs) are increasingly used for visual analysis of topography, landforms, as well as modeling of surface processes (Sharma and Kujur, 2012). This study used high-resolution DEM and google earth for identification of different geomorphic units. In the beginning, the whole image of the study area has been classified by keeping the physiography and relief as criteria. Then, five geomorphic units have been mapped based on the landform characteristics, slope, their aerial extent etc. The geomorphic units that have been identified and mapped (Figure 3.14) include smooth plain, irregular plain, escarpment, hills and mountains. The different geomorphic units of the study area are illustrated in (Table 3.13) and reclassified as per suitability rank of groundwater existence.

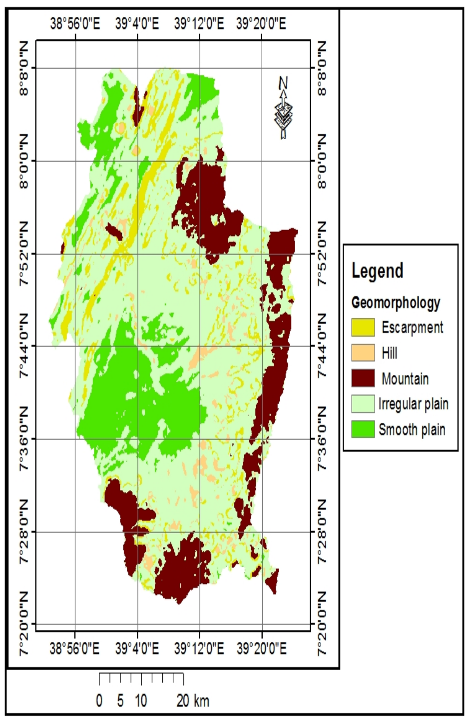

Figure 3.14: Geomorphology of the study area

Table 3.13: Geomorphology suitability for identification of groundwater potential zones

Factors	Landform types	Rank	Classification
Geomorphology	Mountain, hill and escarpment	2	poor

	Irregular plain	4	Good
	Smooth plain	5	Very good

Source: (Abdul-Aziz Hussein *et al*, 2016).

3.4.2.9 Soil Moisture

The backscattering coefficient of Sentinel-1A was analyzed and compared to the Normalized Vegetation Index (NDVI) calculated from sentinel-2A. NDVI (Figure 3.15) has been widely applied in monitoring various vegetation cover. This index is frequently used as a proxy for plant growth and productivity. The amount of solar radiation reflected by the vegetation canopy is related to wavelength, chlorophyll, leaf interior tissues and plant water content. The relative soil moisture content from Sentinel-1A was qualitatively estimated from backscattering coefficient expressed in dB. The soil moisture in the positive processed image appears lighter, which has high decibel value. However, built-up areas have higher decibel value due to high electromagnetic diffusion of metals on the roofs. All pixels, which have greater than -13 dB and smaller NDVI value are necessarily built-up areas (Mansaray, 2017). Due to this, built-up areas were masked and were given lower weight for groundwater exploration. Areas which have high decibel value and high NDVI value have high soil moisture content, which is suitable for potential groundwater exploration. The dB value of the current study ranges from -28 to 9.7 dB. The dB value was classified into four to identify soil moisture zones. The soil moisture zones were reclassified as per suitability rank of groundwater occurrence (Table 3.14).

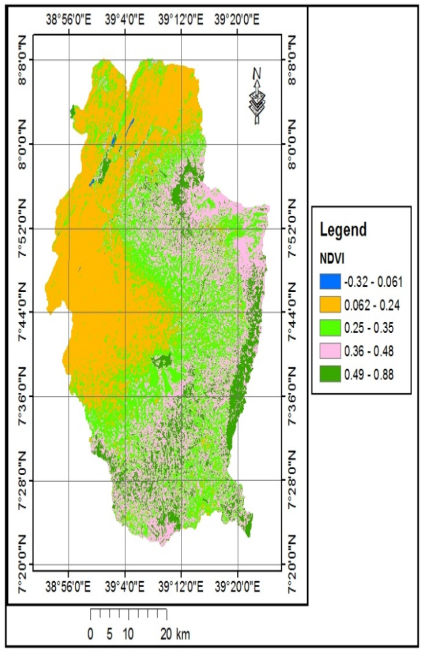

Figure 3.15: Normalized Vegetation Index of the study area

Table 3.14: Soil moisture suitability for identification of groundwater potential zones

Factor	Class (dB)	Rank	Classification
Soil moisture (dB)	<-22	2	Poor
	-22 – -18	3	Moderate
	-18 – -13	5	Very good
	>-13	2	Poor

3.5 Analytical Hierarchy Process

Analytic hierarchy process (AHP) is one of the most effective Multi-Criteria Decision Making (MCDM) techniques which helps to make a decision when facing complex problems (Zeinolabedini and Esmaeily, 2015). The method was stated by Satty (1980) in four steps. The method includes problem modeling and making hierarchical structure, pairwise comparison, evaluating weight and combining weights. Analytical Hierarchy Process is the method which is used to determine the weights of many factors for identifying the groundwater potential zones based on weights assignment and normalization with respect to the relative contribution of the different themes to groundwater occurrence (Jhariya *et al*, 2016). Analytical Hierarchy Process calculates the required weights associated with the respective criterion map layers. The method calculates with the help of a preference matrix, in which all relevant criteria identified are compared against each other and aggregated the weights.

3.5.1 Establishing Decision Hierarchy

The decision hierarchy model of groundwater potential zones structured (Figure 3.16) consists of the main objective at the top (GWPZ), followed by three levels of hierarchy. The nine criteria (also known as factors) used in this research were divided into two main groups; environmental and hydrological factors. These were also further split into factors of which, four were environmental (topography, geology, soil and LU/LC) and two were hydrological (drainage density and rainfall). The final hierarchy was formed by dividing the topography, geology and soil factors. Topography divided into slope and geomorphology sub-factors and geology was divided into two sub-factors of geological unit and lineaments density. Soil was divided in to soil texture and soil moisture sub-factors. The examined criteria were selected based on the relevant literature for specific major study area problem. In a complete hierarchy, every layer in the lower hierarchical level affects every element in the upper hierarchical level. Therefore, the elements in the lower hierarchical level were then compared to each other based on their effect on the major influential layer above.

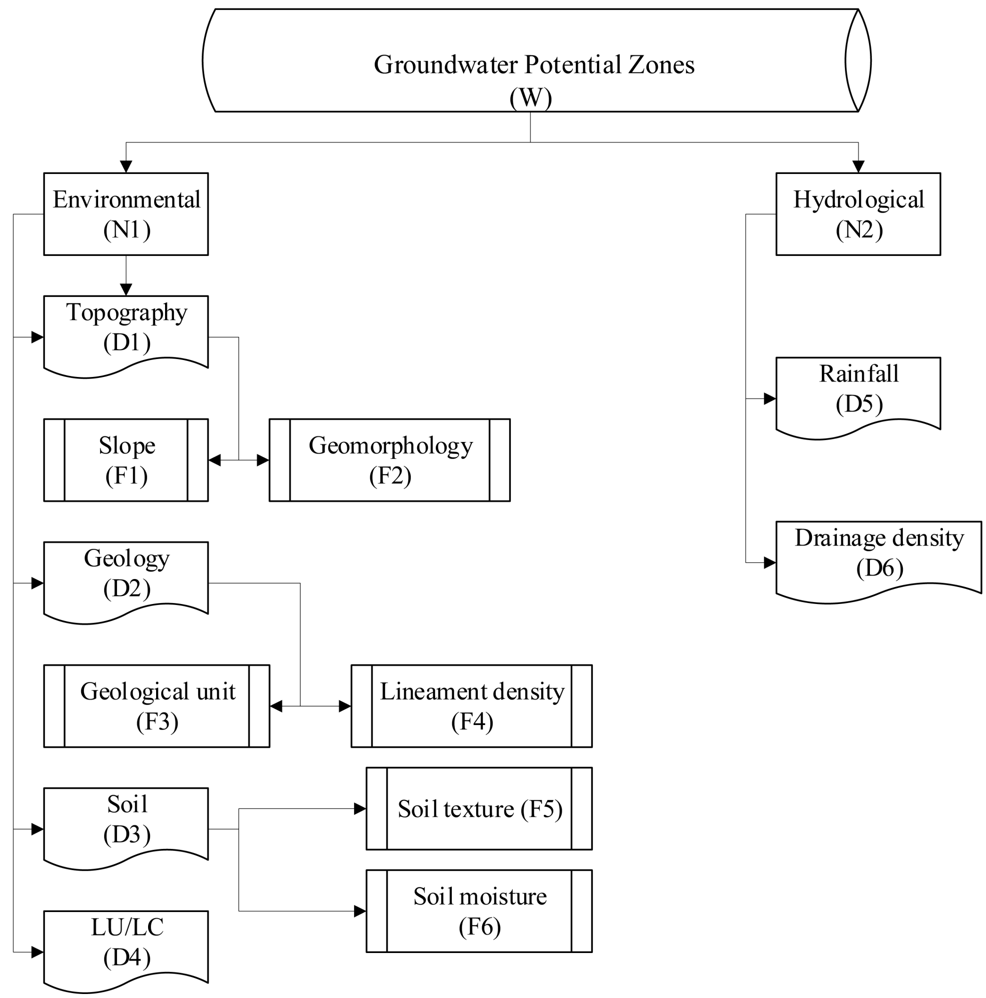

Figure 3.16: Hierarchical decision analysis

3.5.2 Pairwise comparison

Reclassification and ranking were done to each criterion layers in section 4.2 for determination of their relative importance. The reclassified criteria layers had their own influence on the outcome, through a quantitative rank. Pairwise comparison method was used for the assignment of weight for criteria layers. Pairwise comparison matrices were created for each of the lower hierarchical levels one matrix for each element in the level immediately above. This was done by considering which layer effect is dominant than the other. The pairwise comparison matrices were formed by interviews conducted with various experts and knowledge of the researcher. A pairwise comparison matrix is derived using Satty's (1980) nine-point importance scale. The relative importance values are determined with 1–9 scale (Table 3.15), in which a score of 1 represents equal importance between the two themes and a score of 9 indicates the extreme importance of one theme compared to the other one. Satty (2008) suggested that a nine-point scale with ranges between 1.1 and 1.9 to compare alternatives that differ slightly.

Table 3.15: Scale of relative importance

Scale	Definition
1	Equal importance
2	Weakly importance
3	Moderate importance
4	Moderate plus
5	Strong importance
6	Strong plus
7	Very strong importance
8	Very, very strong
9	Extreme importance
1.1–1.9	The factors are closely importance

Source: (Satty, 1980 and 2008).

Framing the pairwise comparison

The importance of each pair of criteria is compared with respect to the goal of the decision problem (groundwater potential zone in this case). The important thing here is that, considering which criteria are more important than others. The rank given for higher and lower criteria in hierarchical decision model (Figure 3.16) was given by using Sat's nine-point scale. The scale for each factor was given by looking real problems and considering the role of each criterion for the occurrence of groundwater. Elements of the matrix in each level are compared in pairs with respect to their importance to the element in the next higher level. Starting at the top of the hierarchy and working down, the pair-wise comparison square matrixes are formed such that all the elements in the matrix are positive as given in equation (4).

(4)

Such that [aij]> 0

The diagonal elements of the square matrix are always 1 because the same factors have the same weight. Therefore, the upper triangular and lower triangular matrix should be made by comparing the factors with each other. The matrix generally has the property of reciprocity, which is expressed mathematically for n numbers of elements in pairwise comparison matrix. The lower triangular matrix is filled using equation (5).

(5)

Then, each element of the column of the matrix are summed up and each element of the column are divided with the sum of its column to get the normalized relative weight using equation (6).

(6)

Where n is the number of elements of a column and is normalized weight.

Then, the weights of the pairwise matrix are calculated by taking an average of the normalized relative weights in a row for each class within a factor related to higher hierarchy as given in equation (7)**.**

for all i=1,2…n (7).

3.5.3 Evaluation of Matrix Consistency

The value of pairwise comparison matrix relies on the subjective judgment which might lead to an arbitrary result with bias. Due to this, pairwise comparison matrix evaluation is needed. The AHP consistency ratio method was used to determine whether the weight criteria layers are consistent or not. Satty (1980) gave a measure of consistency, called Consistency Index as deviation or degree of consistency using equation (8).

, where is the largest eigenvalue, and N is the order of comparison matrix (8)

Using weighted sum and priority, λmax is calculated using equation (9).

, where is the order of comparison matrix (9)

Then, the efficiency criteria are measured using consistency ratio (CR) as given equation (10)

, where RI is the Random consistency indices. (10)

The Random Consistency Indices is given by Satty (1980) which is illustrated in (Table 3.16).

Table 3.16: Random consistency indices (Satty, 1980)

N	1	2	3	4	5	6	7	8	9
RI	0	0	0.58	0.90	1.12	1.24	1.32	1.41	1.45

When CR>0.1, there is an indicator of error when assigning ranks to the criteria/factors. Due to this, it should reevaluate the assigning relative importance of the factors. On the contrary, when CR<0.1, the overall of assigning weights for each factor is acceptable for decision making.

3.5.4 Calculating the Final Weight of Each Criteria Layers

The weight final (Wf) of every criteria layer to the main objective of the decisional hierarchy (groundwater potential zone) was calculated by normalizing the weight (w) of each factor. This was done by multiplying the weight of a factor in the lower level by that of the weights of elements in the upper level if and only if when they are in the same decisional hierarchical family. For instance, the final weight of lineament density (LD) was calculated as;

Final weight of LD = weight of environment (N1) * weight of geology (D2) * weight of LD (F4)

This method was used for all final weights of each criteria layer, in which the sum of all final weights of criteria layers is equal to one.

3.5.5 Groundwater Potential Zone identification based on Criteria Weights

One of the most important applications of GIS is that of decision support. IDRISI software is very important to specifically address multi-objective, multi-criteria resource allocation decision problems, as well as problems of assessing and incorporating uncertainty in the decision-making process. For the current study, the weighted linear combination was used in which, reclassified factors are combined by applying a weight to each followed by a summation of the results to yield groundwater potential zones map as stated in equation (11).

(11)

Where is Ground Water Potential Zones, is the weight of factor and is criterion score of factor .

3.6 Validation of Groundwater Potential Zones

The potential groundwater zones were validated based on water point inventory data of boreholes, hand-dug wells and springs. The accuracy of the identified potential zones is estimated based on total number of validation data and the total number of disagreement data (as stated in equation (12) with their actual yield (Jhariya et al, 2016).

(12)

Where, is groundwater potential zones and is number of validation.

CHAPTER FOUR

4 RESULTS

4.1 Pre-processing and Processing Products of Optical and RADAR Sentinel data

Pre-processing products of MSI Sentinel-2A (Figure 4.1c) and RADAR Sentinel-1A (Figure 4.1a) showed that the images are readymade for further processing of thematic layer derivations (section 3.4.2.6–3.4.2.9). Digital Elevation Model (Figure 4.1b) was generated from SAR Sentinel-1A, which has the same resolution with the processed SAR image. The processed Sentinel-1A SAR image is presented as a grey scale, with the intensity of each pixel representing the amount of energy returned from that area on the ground. Backscatter coefficient (σ°) in decibels (dB) represents target backscattering area per unit ground area. The positive number in backscattered coefficient is a focusing of backscattered energy towards the RADAR, and a negative number is a focusing of backscattered energy away from the RADAR. Positive values in the processed image of Sentinel-1A are almost for densely built-up urban areas where double bouncing reflectance is common in such areas.

4.2 Reclassified Thematic Layers (Factors)

The groundwater potential zone map of the current study was identified by using standardized layers from processed products of Sentinel-1A, Sentinel-2A and with existing collateral data. The nine identified thematic layers in section 3.4.2 were reclassified based on standardized criteria.

4.2.1 Reclassified Land-use/Land-cover

Different types of LU/LC have a different rate of occurrence of groundwater due to different infiltration ability. Considering this, LU/LC of the study area was reclassified (Figure 4.1d) based on suitability rank in section 3.4.2.7. The reclassified LU/LC result showed that highest area of coverage (75.83%) of the total study area is moderately suitable (Table 4.1) for identification of groundwater potential zones.

Table 4.1: Area coverage of Reclassified Land-use/Land-cover

Suitability	Rank	Area (km^2)	Area (%)
Very poor	1	327.83	9.78
Poor	2	354.26	10.56
Moderate	3	2543.27	75.83
Good	4	109.08	3.25
Very good	5	19.56	0.58

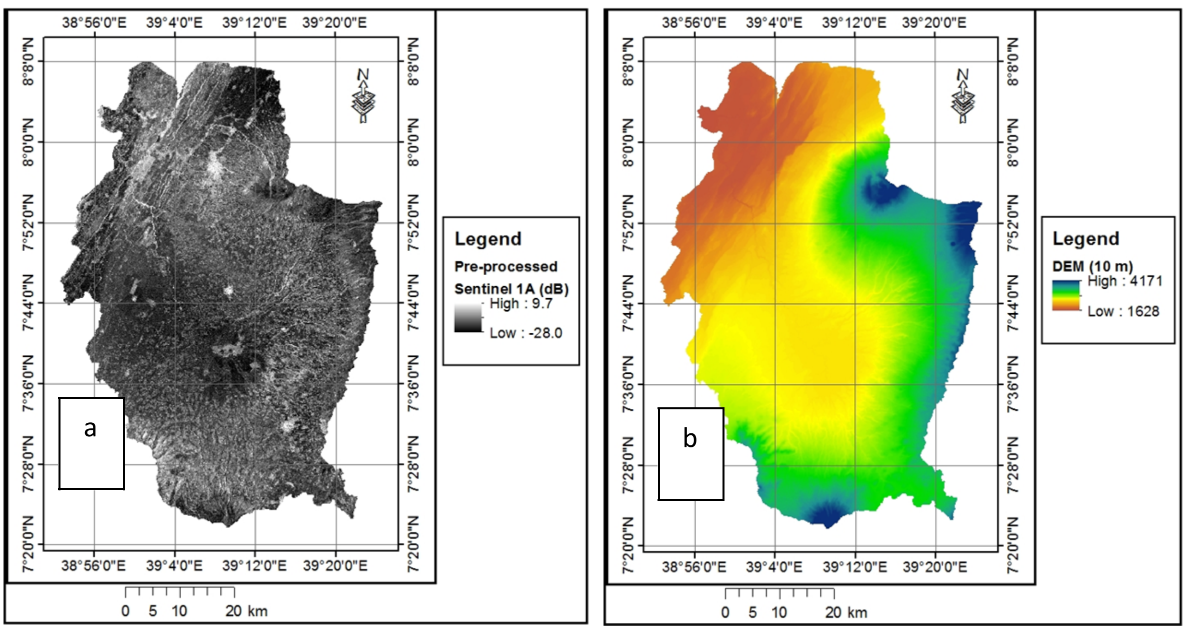

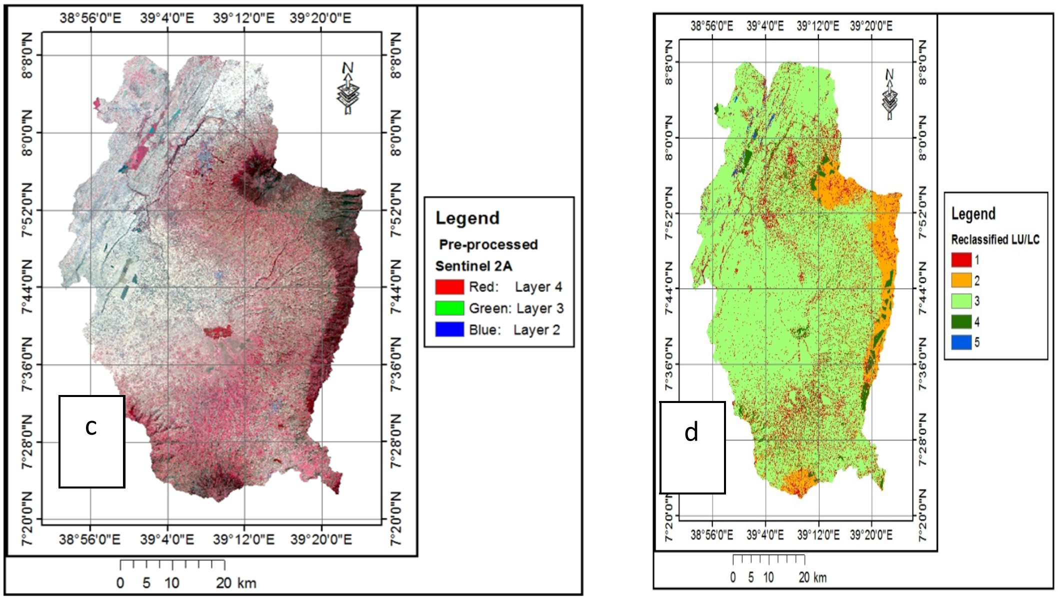

Figure 4.1: Pre-processed Sentinel-1A (a), Digital Elevation Model (b), Pre-processed Sentinel-2A (c) and Reclassified Land-use/Land-cover (d)

4.2.2 Reclassified Slope

The slope in the study area was reclassified (Figure 4.2a) based on suitability rank (section 3.4.2.1) for identification of groundwater potential zones. Areas around Lake Ziway and western part of Sagure have leveled to gentle slope and areas of eastern and southern are mountainous, which have steep to the very steep slope. Flat and gentle slope areas are suitable for the occurrence of very high and high groundwater. On the contrary, steep slope areas have least role due to high runoff.

4.2.3 Reclassified Drainage Density

The reclassified drainage density (Figure 4.2b) indicated that, as drainage density increases the potentiality to occur groundwater decreases. The higher the drainage density of the study area results the higher the runoff. Areas of least drainage densities indicated good areas for the occurrence of groundwater and vice versa.

4.2.4 Reclassified Geological units

The geological units in the present study were reclassified (Figure 4.2c) based on the degree of fracturing (primary and secondary porosity) as stated in section 3.4.2.3. The more fractures are found in northwest part of the study area, which are very good areas for the occurrence of groundwater. From the total study area, very poor class of reclassified geological unit has the highest area coverage (Table 4.2).

Table 4.2: Area coverage of Reclassified geological units

Suitability	**Rank**	**Area (km^2)**	**Area (%)**
Very poor	1	1508	44.96
Poor	2	410	12.22
Moderate	3	594	17.71
Good	4	305	9.1
Very good	5	537	16.01

4.2.5 Reclassified Lineament Density

The reclassified lineament density (Figure 4.2d) of the study area indicated that the higher the lineament density is the more occurrence of groundwater. Therefore, based on suitability rank in section 3.4.2.6, the high lineament densities in the northwest part of the study area has a high rate for the existence of groundwater.

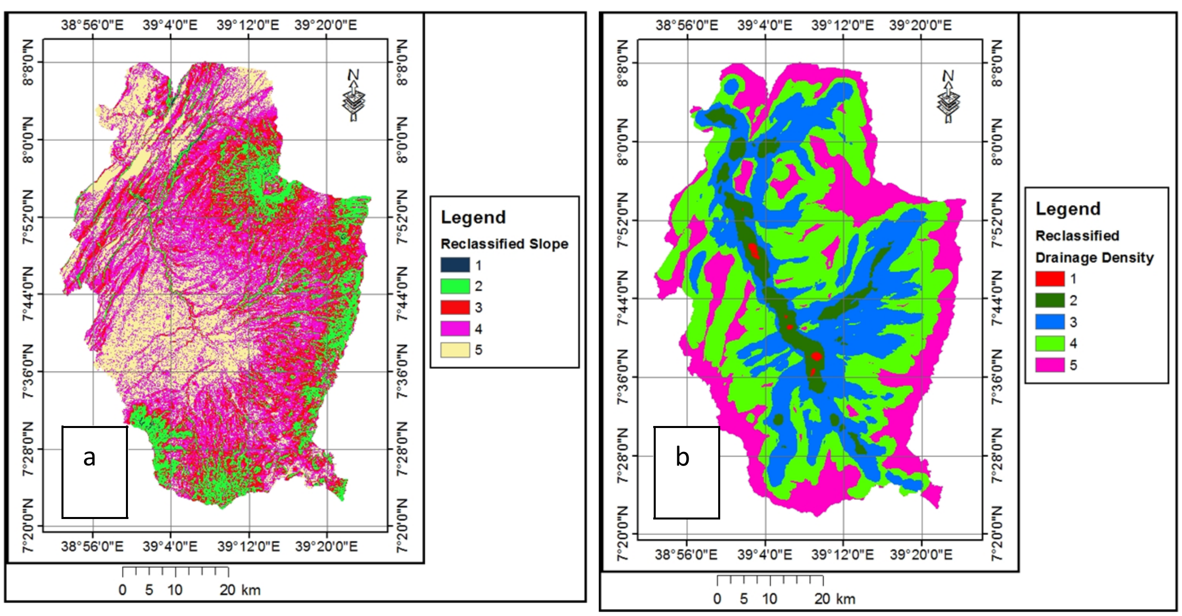

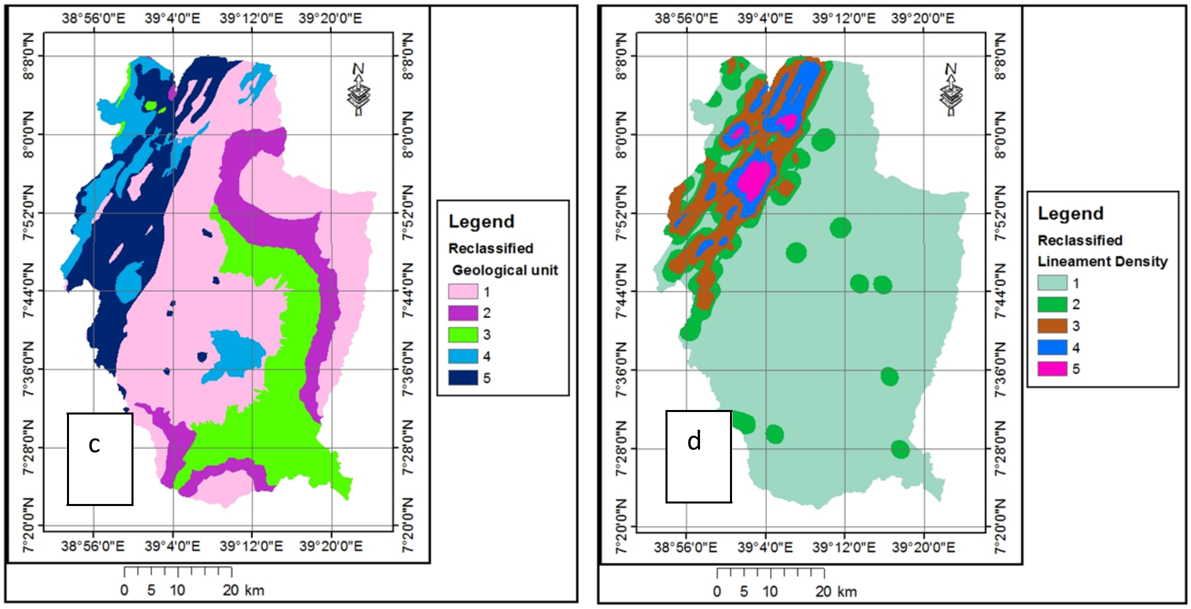

Figure 4.2: Reclassified factors of Slope (a), Drainage density (b), Geological unit (c) and Lineament density (d)

4.2.6 Reclassified Soil Texture

The reclassified soil texture factor map (Figure 4.3a) indicated that around Lake Ziway (northwest) part of the area has a coarse grain texture soil type (sandy loam and loamy sand), which is suitable for water infiltration. The clay and loam soil in middle and eastern part of the study area are poor and moderately suitable for water infiltration. From total area of reclassified soil texture, the very poor zone has the highest area of coverage 51.15%.

The moderate zone covers 47.34% of the study area. Good and very good suitability class covers 1.46% and 0.05% of the total study area respectively.

4.2.7 Reclassified Rainfall

The reclassified mean annual rainfall of the study area (Figure 4.3b) has a significant role for the occurrence of groundwater because rainfall is the source of groundwater directly or indirectly. The high rainfall areas are in highlands of mountains areas. Small rainfall was observed in and around rift floor areas. Based on suitability rank in section 3.4.2.5, the high rainfall areas were reclassified as very good to moderate zones for groundwater exploration, and small rainfall areas were reclassified very poor zone.

4.2.8 Reclassified Soil Moisture

The soil moisture zones of the study area were reclassified (Figure 4.3c) as per suitability rank of groundwater occurrence. Areas which have high decibel value and high NDVI value have high soil moisture content, which is suitable for groundwater exploration. Very good zones of reclassified soil moisture cover 6.32% of the total study area. Moderate and poor zones cover 50.66% and 43.02% respectively.

4.2.9 Reclassified Geomorphology

The different geomorphic units of the study area described in section 3.4.2.8 were reclassified (Figure 4.3d) as per suitability rank of groundwater occurrence. The reclassified geomorphology result has shown that Smooth plain and irregular plain areas were suitable areas for the existence of groundwater based on criteria ranks in section 3.4.2.8. Hills, escarpments and mountains areas are poor areas for groundwater existence. Eastern and southern areas of the study area are mountainous areas, which was reclassified as poor zones for the occurrence of groundwater. The area coverage of each suitability class from the total study area is presented in (Table 4.3).

Table 4.3: Area coverage of Reclassified Geomorphology

Suitability	**Rank**	**Area (km^2)**	**Area (%)**
Poor	2	886	26.42
Good	4	1916	57.13
Very good	5	552	16.45

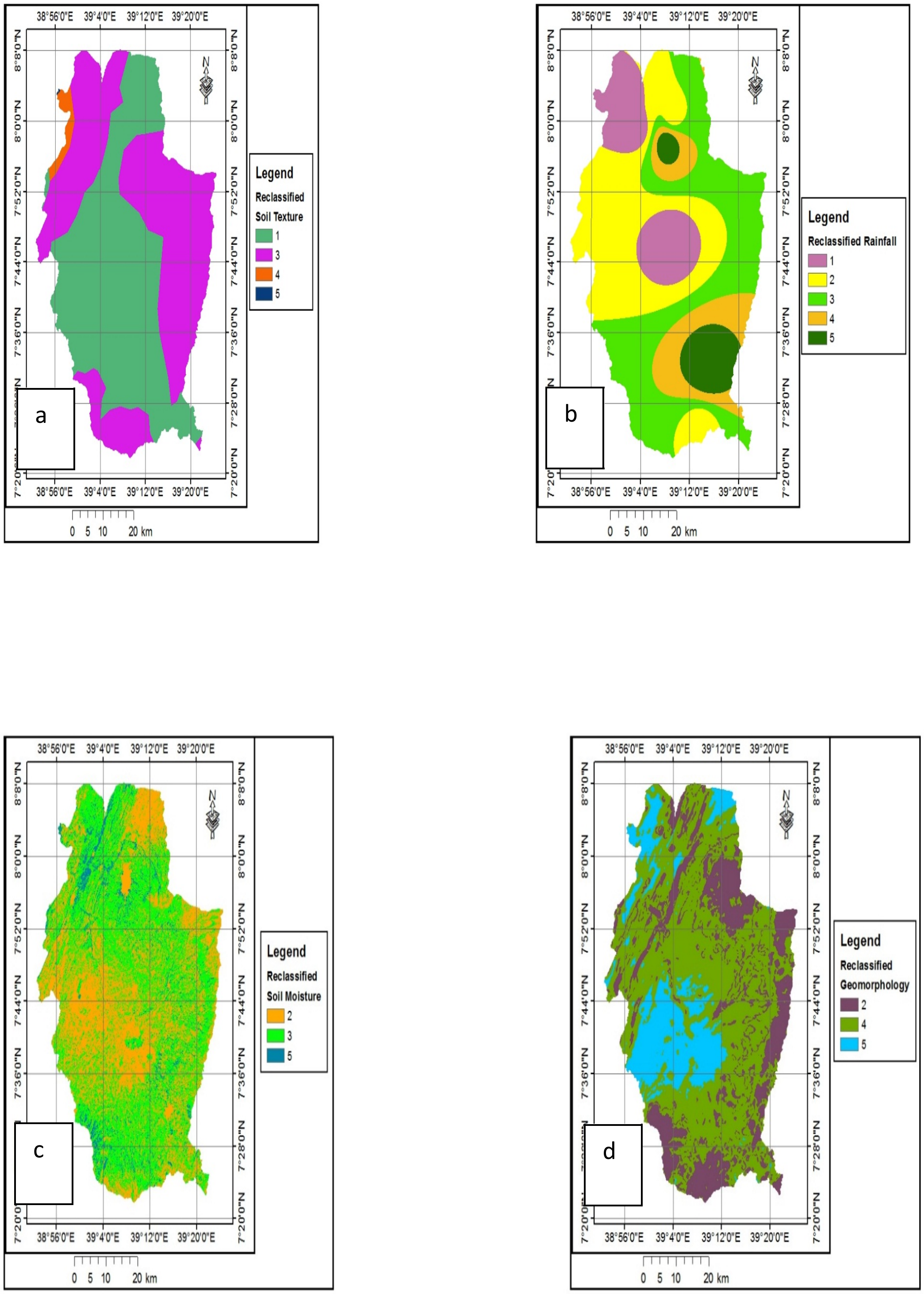

Figure 4.3: Reclassified factors of Soil texture (a), Rainfall (b), Soil moisture (c) and Geomorphology (d).

4.3 Weight of Main factors, Factors and Sub-factors

The pairwise comparison of main criteria (Table 4.4) in the higher hierarchy (environmental to that of hydrological) showed that environmental is moderately importance than hydrological. This is because of the storage and movement of groundwater is mainly controlled by environmental factors. The rank of hydrological factor has the reciprocal of an environmental factor as stated in equation (5) in section 3.5.2. The comparison matrix of environmental factors is illustrated in (Table 4.5). The weight of main factors, factors, and sub-factors (Table 4.4, 4.7, 4.10, 4.11, 4.12 and 4.13) was derived using a normalized matrix based on equation (6 and 7) in section 3.5.2. The CR value of two comparison matrix is 0.0 due to the value of RI.

Table 4.4: Pairwise comparison matrix of main factors

Groundwater Potential	Environment	Hydrology	**Weight**
Environment	1	3	0.75
Hydrology	1/3	1	0.25

Table 4.5: Comparison matrix of Environmental factors

Environment	Geology	Topography	Soil	LU/LC
Geology	1	2	2	6
Topography	1/2	1	3/2	4
Soil	1/2	2/3	1	4
LU/LC	1/6	1/4	1/4	1
Sum	2.167	3.92	4.75	15

The normalized matrix was computed based on equation (6), each element of the column of the matrix are summed up and each element of the column are divided with the sum of its column to get the normalized relative weight (Table 4.6)

Table 4.6: Normalized matrix of Environmental factors

Environment	Geology	Topography	Soil	LU/LC
Geology	0.461	0.510	0.421	0.4
Topography	0.231	0.255	0.316	0.267
Soil	0.231	0.171	0.211	0.267
LU/LC	0.077	0.064	0.052	0.066

Table 4.7: Priorities (Weights) of Environmental factors

Environment	Geology	Topography	Soil	LU/LC	**Priority (Weight)**

Geology	0.461	0.510	0.421	0.4	0.448
Topography	0.231	0.255	0.316	0.267	0.267
Soil	0.231	0.171	0.211	0.267	0.22
LU/LC	0.077	0.064	0.052	0.066	0.065
		Sum			1

After deriving priorities, matrix consistency evaluation is very crucial to check the ranks that were given for each criterion is acceptable or not. The matrix consistency evaluation for environmental factors was evaluated based on priorities and weighted sum (Table 4.8 and Table 4.9).

Table 4.8: Weighted columns of Environmental factors

Environment	Geology	Topography	Soil	LU/LC
Geology	0.448	0.534	0.44	0.39
Topography	0.224	0.267	0.33	0.26
Soil	0.224	0.179	0.22	0.26
LU/LC	0.075	0.067	0.055	0.065

Table 4.9: Weighted Sum of Environmental factors

Environment	Geology	Topography	Soil	LU/LC	**Weighted Sum**
Geology	0.448	0.534	0.44	0.39	1.812
Topography	0.224	0.267	0.33	0.26	1.081
Soil	0.224	0.179	0.22	0.26	0.883
LU/LC	0.075	0.067	0.055	0.065	0.262

Based on weighted sum and priority, λmax was calculated using equation (9), which is =4.035. The consistency index was computed based on equation (8), which results in CI = 0.012. Then, consistency ratio was computed as per equation (10) and the computed result of CR = 0.013. Since the value of CR = 0.013 is less than 0.10, it was assumed that the judgments matrix is reasonably consistent to continue the process of decision-making using AHP.

Table 4.10: Pairwise comparison matrix of topographic sub-factors.

Topography	Slope	Geomorphology	**Weight**
Slope	1	3	0.75
Geomorphology	1/3	1	0.25

Table 4.11: Pairwise comparison matrix of Geology sub-factors

Geology	Geological unit	Lineament	**Weight**
Geological unit	1	3	0.75
Lineament	1/3	1	0.25

Table 4.12: Pairwise comparison matrix of Soil sub-factors

Soil	Soil texture	Soil moisture	**Weight**
Soil texture	1	7	0.875
Soil moisture	1/7	1	0.13

Table 4.13: Pairwise comparison matrix of hydrological factors

Hydrology	Rainfall	Drainage density	**Weight**
Rainfall	1	7	0.875
Drainage density	1/7	1	0.125

4.4 Final Weight of Thematic Layers

The result of the final calculated factors weight (Table 4.14) showed that geology and rainfall is the dominant factor followed by soil texture, slope, lineament density, geomorphology, LU/LC, drainage density and soil moisture respectively.

Table 4.14: Weights of main criteria, criteria, sub-criteria and final weights of each criterion

Main criteria	**Weight**	**CR**	**Criteria**	**Weight**	**CR**	**Sub-criteria**	**Weight**	**CR**	**Final weight (N*D*F)**	**%**
N1	0.75	0.00	D1	0.267	0.013	F1	0.67	0.0	0.13	13
						F2	0.33	0.0	0.07	7
			D2	0.448	0.013	F3	0.67	0.0	0.23	23
						F4	0.33	0.0	0.11	11
			D3	0.22	0.013	F5	0.875	0.0	0.14	14
						F6	0.125	0.0	0.02	2
			D4	0.065	0.013				0.05	5
N2	0.25	0.00	D5	0.875	0.0				0.22	22
			D6	0.125	0.0				0.03	3
				Total					1	100

Where N1 = environmental main factor, which includes D1 = topography, D2 = geology, D3 = soil and D4 = LU/LC. F1 and F2 are slope and geomorphology within topography. F3 and F4 are geological unit and lineament density in geology factor. F5 and F6 are soil texture and soil moisture in soil factor. N2 is a hydrological main factor, which includes rainfall (D5) and drainage density (D6).

4.5 Identified Groundwater Potential Zones

The groundwater potential zones of the study area were identified by using WLC of the nine reclassified thematic layers with their percentage of influence by using equation (11) in section 3.5.5. The result of groundwater potential zones (Figure 4.4) has five suitability classes, which are very low, low, moderate, high and very high. From the total study area, the very high zone has the smallest area of coverage (428.23 km^2) and the low zone has the highest area of coverage (942.19 km^2) relative to others (Table 4.15) and (Figure 4.5).

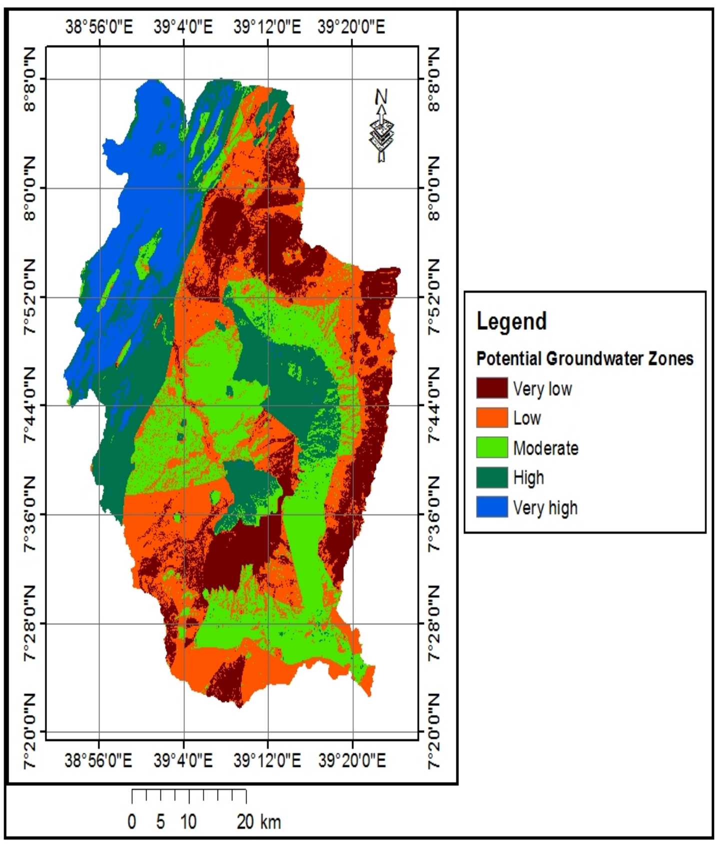

Figure 4.4: Identified Groundwater Potential Zones

Table 4.15: Area coverage of Identified Groundwater Potential Zones

Potential Groundwater Zones	**Area (km^2)**	**Area (%)**
Very low	607.64	18.12
Low	942.19	28.1
Moderate	777.2	23.17
High	598.74	17.85
Very high	428.23	12.76

Figure 4.5: Area coverage of Identified Potential Groundwater Zones

4.6 Validation of Identified Groundwater Potential Zones

The zonation of groundwater potential by using optical and RADAR microwave remote sensing with existing collateral data was a close agreement with the existing point source inventory data. The point data of boreholes, dug wells, and springs were overlaid on the result of potential groundwater zone map (Figure 4.6) and they coincide with the expected values. From the total wells and springs in the very high potential zone, 14 validation points have a high yield (2.5–25 l/sec.). One deep borehole (250 m) in the north part of Assela, is located in the very low potential zone, which has no water (yield). This indicates that the well site is not good for groundwater exploitation. Two boreholes, one dug well and four springs which have 2–20 l/sec. were observed in high potential groundwater zone. However, one dug well, which has a low yield (0.25 l/sec.) is observed in the high potential zone. This is mainly due to shallow depth or less degree of fracturing in contacts to different rocks. Most springs observed in the study area are located in the moderate potential zones following the same altitude. Ten springs which have a yield of (0.5–15 l/sec.) were overlaid in the moderate zone. Two hand dug wells and two springs, which have less yield (0.17–0.5) were overlaid in low potential zones. One hand dug well and five springs were overlaid in very low potential zones in which their yield ranges (0.17–0.3 l/sec.). Most wells are observed in high and very high potential zones in the north-west part of the study area.

These wells have high yield due to more fractures overlaid in igneous rocks (ignimbrites, and recent-basalts) and in lacustrine sediments. The accuracy of prediction is illustrated in (Table 4.16).

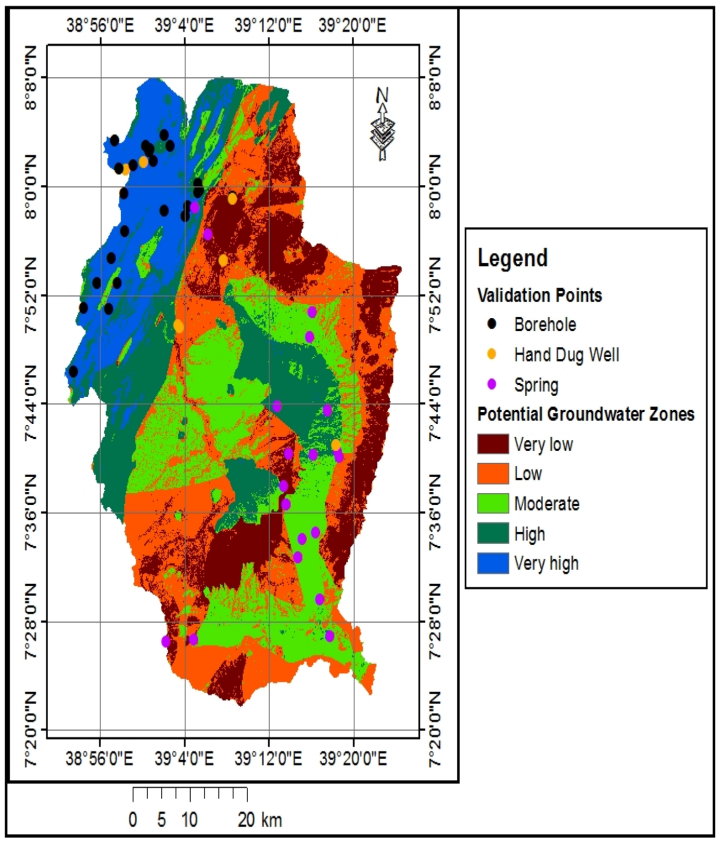

Figure 4.6: Validation of Identified Groundwater Potential Zones

Table 4.16: Validation of Identified Potential Groundwater Zones with actual yield

No.	Groundwater zone validation data	Very high	High	Moderate	Low	Very low
1	Total no. of validation data under different GWPZ	14	7	10	5	7

2	No. of validation points under agreement	13	6	10	4	7
3	No. of validation points under dis-agreement	1	1	-	1	-
4	Highest yield in agreement (l/sec.)	25	20	15	0.5	0.3
5	Yield in dis agreement (l/sec.)	2.5	0.25	-	1	

The accuracy of the identified potential zones is estimated based on total number of validation and disagreement data. Total number of validation data = 43 and the total number of water point inventory data where there is an agreement between the expected and the actual yield = 40; number of data, where there is a disagreement between the expected and the actual yield = 3. Then, the accuracy of prediction is calculated based on equation (12) in section 3.6, and the computed result shows 93%. The prediction accuracy obtained (93%) showed that the method applied for this research produced significant and reliable results.

CHAPTER FIVE

5 DISCUSSION

GIS and remote sensing technologies are used for analysis and integration of several surface features that are used to indicate groundwater potentialities systematically at least cost and short time (Oh *et al*., 2011). Integrated optical and RADAR sentinel family, which are used for this study, has a significant role in the identification of groundwater zones. Sentinel-1A images were used for identifying structures, which are very important for the movement of groundwater. High-resolution DEM was generated from sentinel-1A while geometric correction after image calibration and speckle filtering. From high-resolution DEM, factors of Slope, geomorphology, lineament density and drainage density were clearly identified and used for groundwater investigation. The occurrence and movement of groundwater are controlled by various factors, and each factor has its own weight depending on their influence on the movement and storage of groundwater. The potential groundwater zones map (Figure 4.4) in the present study was identified based on the weight of nine thematic layers (geological unit type, lineament density, rainfall, drainage density, slope, geomorphology, soil texture, soil moisture and LU/LC). All those factors do not have equal importance in controlling groundwater. Due to this, weighted value determination is very important after all thematic maps were organized (Abdul-Aziz Hussein *et al*., 2016). The weights of each criterion were derived by using AHP techniques as many studies were assessed by this technique (Fashea, 2014; Abdul-Azzi Hussein *et al*., 2016; Das, 2017). Saaty (1980) clearly describes the range of inconsistency, which should be less than 0.1 in weight comparison analysis. While deriving the weight of each factor in the present study, the CR value was 0.013 which is less than 0.1 and it is acceptable for further analysis.

The occurrence and movement of groundwater in a certain area of a hard rock landscape are mainly controlled by secondary porosity triggered by the fracturing of the underlying rocks. In the rift floor part of the study area, more fractures /lineaments/ are observed underlying on the rocks of recent-basalts and ignimbrites which are caused for the existence of high storage of groundwater (Astatke Kiflu *et al*., 2002). Very high groundwater zone in this study was identified around high fractures overlaid in ignimbrites and basalts. Additionally, very high and high potential zones were identified in lacustrine sediments and in alluvial deposits due to their primary porosity.

Low and very low potential zones in the area were observed in pumice, tuff and trachyte type of geological unit. Due to its high control for the storage and movement of groundwater, the weight given for geology was higher than others (Abdul-Aziz Hussein *et al*., 2016). In the present study, the weight influence of geology has given high weight (34%), which is a combination of geological unit type (23%) and lineament density (11%).

There are many sources of recharges to groundwater systems. These include recharge from precipitation, rivers, irrigation losses, urban water sources and inter-aquifer flows (Tenalem Ayenew, 1998). According to Tenalem Ayenew (1998), Highland stations with complete wet season rainfall records were correlated with discharge for the corresponding months. This indicates that summer highland rainfall has an important control over discharge and lake levels in the rift. In this study, from 30-year precipitation data, highest rainfall was observed in the highlands, which are the main recharge areas. The recharged rainfall flow to lowlands (discharge areas) due to topographic effect via interconnected pores, open joints, and fissures. High weight next to geology was given for rainfall (22%). However, due to topographic, and other thematic layer effects, high rainfall areas were resulted in very low to moderate potential zones. Unlike lowland areas, drainages in high lands are susceptible to runoff than infiltration causes to have high drainage density in highlands (Tenalem Ayenew, 1998). The higher the drainage density is the lower infiltration, which results in the occurrence of the lower potential zone and the reverse is true. The assigned weight for drainage density was 3%. Drainage density has lower influence on the existence of groundwater (Barik *et al*., 2017).

Topography has a great role in the occurrence of groundwater. The total weight for topography was given 20%, which is a combination of slope (13%) and geomorphology (7%). Slopes are a major governing factor for groundwater. The steep slope allows the rainwater to runoff, and level to gentle slope region permits the rainwater to infiltrate to the soil (Ibrahim-Bathis and Ahmed, 2016). In the mountains, steep slopes and hill areas of the study area, the resulted groundwater zones are very low to low. The very high and high groundwater potential zones are mostly in the alluvial plains/valleys, with smooth and irregular plain geomorphological classes (Abdul-Aziz Hussein *et al*., 2016).

In this study, high and moderate potential groundwater zone was observed in irregular plain landforms. The very high potential zone was in smooth/ flat plains in the rift floor part of the study area. The soil is an important factor for recharging purpose because the rate of infiltration depends on the grain size and related hydraulic characteristics of the soils (Fashae *et al*., 2014). The total weight assigned for soil was 16 %, which is a combination of 14% for soil texture and 2 % for soil moisture. The compact clay soil type has less role for the existence of high groundwater because it holds the water than to allow penetration (Ibrahim-Bathis and Ahmed, 2016). Clay soil type in the middle of the study area was one of the main effects for the existence of low potential zone. A coarse-grained size soil texture around lake Ziway, like loamy sand and sandy loam with high soil moisture, is resulted to have a high to very high potential groundwater zone in that area. However, even if the soil moisture is high around kakka mountain, the groundwater zone is very low to low due to clay soil texture. In addition to soil, LU/LC has a significant role in infiltration. According to Das (2017) wetlands, forests and cultivated land-covers have good groundwater potential. These land-covers for this study have a significant role in the existence of high groundwater. According to Damtew Fufa (2015), LU/LC change from 1986 to 2010 have shown the overall increase of farmland, and reduction of natural forest and grassland in Ketar watershed. Deforestation of natural forest and increase in farmland was manifested by the rapid increase in human population, which affects the whole watershed. In this study, most part of the area is covered by farmland. The increment of farmland is directly related to the need of water availability for irrigation.

The weight calculated from AHP comparison was aggregated using WLC based on equation (10) in section 3.5.5. The aggregation output has five potential zones (Figure 4.4), namely very low, low, moderate, high and very high. Many previous studies on groundwater potential zones was validated using existing boreholes, hand-dug wells and springs (e.g. Tesfaye Tessema, 2015; Jhariya *et al*., 2016; Kumar *et al*., 2016; Bari *et al*., 2017; Pinto *et al*., 2017). In the present study, the identified groundwater potential zones were validated by using existing wells and springs. The validation result (93%) showed that the method applied for this research evaluates different factors in detail produced significant, reliable and precise results.

CHAPTER SIX

6 CONCLUSION AND RECOMMENDATIONS

6.1 Conclusion

The identified groundwater potential zones of the study area were the result of integrated optical and RADAR microwave remote sensing with existing collateral data. The pre-processed optical and RADAR sentinel family have a significant role in the identification of potential groundwater zones due to their high spatial resolution (10m). Sentinel-1A SAR image is very important for groundwater investigation because of its high wavelength range with imaging capability day and night in all-weather condition. The longer wavelength C-band SAR has higher ability to penetrate the earth than optical images and used for identifying structures of the earth. These structures have a significant role in the movement of groundwater.

The estimated relative soil moisture from the processed SAR image using relative dB value indicated the performance of RADAR in soil and hydrological applications. The DEM was generated on SAR image, and the layers that were identified from it include Slope, geomorphology, lineament density and drainage density. Land-use Land-cover of the study area was identified on the processed image of Sentinel-2A multispectral instrument. From the total study area, farmland covers most part of the study area (66.86%).

The result of weight comparison of thematic layers showed that geological unit, rainfall, soil texture, slope and lineament density were the major factors for the existence of groundwater. The comparison of thematic layers was based on AHP method using ranks of Saaty's (1980). The result of CR value during comparison was 0.013 which is in an acceptable range.

The groundwater potential zones of the present study were identified by using WLC based on their weight influence and reclassified value of nine thematic layers. The identified groundwater potential zones were very low (18.12%), low (28.1%), moderate (23.17%), high (17.85%) and very high (12.76%). The high and very high potential zones were in high fracture areas of ignimbrites, basalts and also in lacustrine sediments and alluvial deposits.

Level to gentle slope, loamy sand and sandy loam with high soil moisture, farmland, forests, wetlands, waterbodies and less drainage density areas were factors for high and very high potential zones. On the contrary, areas of hills, mountains, steep slopes, clay soil, high drainage density, low lineament density, built up, bare and shrub LU/LC resulted for low and very low potential zones. The high rainfall in highlands (recharge areas) flow to low lands (discharge areas) and control the lake level and groundwater in the rift floor. Finally, the identified potential groundwater zone was validated using existing data of boreholes, hand-dug wells, and springs. The point data of boreholes, hand-dug wells, and springs were overlaid on groundwater potential zones map and they coincide with the expected values with 0.93 correlation. Finally, it can be concluded that integrated optical and RADAR remote sensing with GIS techniques are very efficient, useful, timely and cost-effective tool for resolving water scarcity problems by identifying groundwater potential zones.

6.2 Recommendations

This study recommended that the following should be done in future studies and implementation:

- Detailed soil moisture estimation on RADAR images should be done with integration of field lab data for ground validation.
- Comparison of sentinel-1 polarizations should be done to identify the best polarization that penetrates the earth surface more than other polarizations, and future studies work on the best polarization of Sentinel-1 for detailed analysis of groundwater exploration.

- Considering different types of thematic layers have a significant importance for detailed groundwater identification.
- It is recommended to use high-resolution images for effective groundwater exploration.
- Since this study was based on logical conditions and reasoning, the same method should be applied in other places with appropriate modifications where occurrence and distribution of groundwater are more complex.
- For further validation, well drilling using field geophysical investigations is important on the identified potential zones.

REFERENCES

Abdul-Aziz Hussein, Govindu, V., Amare Gebre and Medhin Niguss (2016). Evaluation of Groundwater potential using geospatial techniques, Northern Ethiopia, Wollo Zone, in Gerardo River Catchment district. *Appl Water Sci*. **7**:2447–2461.

Abraham Mechal, Birk, S., Winkler, G., Wagner., T & Aberra Mogessie (2016). Characterizing regional groundwater flow in the Ethiopian Rift: A multi-model approach applied to Gidabo River Basin, *Austrian Journal of Earth Sciences*. **109** (1): 68–83.

Abuzied, S.M., Yuan, M., Ibrahim, S.K., Kaiser, M.F. & Seleem, T.A. (2016). Delination of Groundwater Potential Zones in Nuweiba area using Remote Sensing and GIS techniques. *International Journal of Processing Systems*. **4** (2): 109–117.

Addabbo, P., Focareta, M., Marcuccio, S., Votto, C., Ullo, S.L. (2016). Contribution of Sentinel-2 data for applications in vegetation monitoring, *Acta IMEKO*. **5** (2): 44–54.

Adiri, Z., El Harti, A., Jellouli, A., Lhissou, R., Maacha, L., Azmi, M., Zouhair, M. and Bachaoui, E. (2017). Comparison of Landsat-8, ASTER and Sentinel 1 satellite remote sensing data in automatic lineaments extraction: A case study of Sidi Flah-Bouskour inlier, Moroccan Anti Atlas. *Advances in Space Research*. **60** (11): 2355–2367.

Alonso-Contes, C.A. (2011). Lineament mapping for groundwater exploration using remotely sensed imagery in a karst terrain, Rio Tanama and Rio de Arecibo basins in the northern karst of Puerto Rico. Unpublish Master's Thesis, Michigan Technological University, 66 pp.

Amitrano, D., Martino, G., Iodice, A., Mitidieri, F., Papa, M.N., Riccio, D. & Ruello, G. (2014). Sentinel-1 for Monitoring Reservoirs: A Performance Analysis. *Remote Sens*. **6**: 10676–10693.

Astatke Kiflu, Yosef Tafa & Yonas Mulugeta (2009). Hydrogeological Mapping of Part of Asela Map Sheet (NB 37-3) South Eastern High Land of Ethiopia. Ministry of Mines and Energy, Geological Survey of Ethiopia. Addis Ababa, Ethiopia**.**

Babu, M., Subramanyam, M.V. & Prasad, G. (2013). Effect of speckle filtering on SAR high resolution data for image fusion. *International Journal of Engineering and Innovative*. **3** (1): 143–153.

Barik, K.K., Dalai, P.C., Goudo, S.P., Panda, S.R. and Nandi, D. (2017). Delineation of Groundwater Potential Zone in Baliguda Block of Kandhamal District, Odisha, India using Geospatial Technology Approach. *International Journal of Advanced Remote Sensing and GIS*. **6** (3): 2068–2079.

Basalfew Zenebe, Mathios Agonafir, Meskerem Teshome, Mekdes Taye, Mekonen Bekele, Mohamed Edris, Getachew Burusa & Ezra Yehualashet (2012). Geology, Geochemistry & Gravity Survey of the Hosaena area. Addis Ababa, Ethiopia.

Bereket Bezabih (2017). Groundwater Potential Mapping using Remote Sensing and GIS in Rift Valley Lakes Basin, Weito Sub Basin, Ethiopia. *International Journal of Scientific & Engineering Research*. **8** (2) :43–50

British Geological Survey (2001). Groundwater Quality in Ethiopia.

CCRS (2013). *Fundamentals of remote sensing*. Natural Resource, Canada.

Central Statistical Agency (2008). Summary and statistical report of the 2007 population and housing census. *Addis Ababa Central Statistical Agency*.

Dagnachew Legesse, Vallet-Coulomb, C. & Gasse, F. (2004). Analysis of the hydrological response of a tropical terminal lake, Lake Abiyata (Main Ethiopian Rift Valley) to changes in climate and human activities. *Hydrological Process*. **18**: 487–504.

Damtew Fufa (2015). Hydrological impacts due to Landuse Landcover Changes of Ketar Watershed, Lake Ziway Catchment, Ethiopia. *International Journal of Civil Engineering and Technology*. **6**(10):36–45.

Das, S. (2017). Delineation of groundwater potential zone in hard rock terrain in Gangajalghati block, Bankura district, India using remote sensing and GIS techniques. *Model. Earth Syst. Environ*. **3**:1589–1599.

Elbeih, S.F. (2015). An overview of integrated remote sensing and GIS for groundwater mapping in Egypt. *Ain Shams Engineering Journal*. **6**: 1–15.

ESA (2014). http://www.esa.int/.

Fashae, O.A., Tijani, M.N., Talabi, A.O., & Adedeji, O.I. (2014). Delineation of groundwater potential zones in the crystalline basement terrain of SW-Nigeria using integrated GIS and remote sensing approach. *Appl Water Sci*. **4**:19–38.

Getachew Haile (2017). Modeling Approach for Identification of Potential Rainwater Harvesting Sites in Arsi Zone, Eastern Ethiopia. Unpublished MSc Thesis, Addis Ababa University, Addis Ababa, Ethiopia, 102 pp.

Getu Tesema (2017). Flood detection and mapping using microwave remote sensing on Lake Koka cachment, Awash River basin. Unpublished MSc Thesis, Addis Ababa University, Addis Ababa, Ethiopia, 88 pp.

Hall, D.K. (1996). Remote sensing applications to hydrology; imaging radar, *Hydrological Sciences*. **41**(4): 609–624.

Horton, R. E. (1945). Erosional development of streams and their drainage basins; hydrophysical approach to quantitative morphology. *Geological society of America bulletin*. **56**(3): 275–370.

Ibrahim-Bathis, K. and Ahmed, S. A. (2016). Geospatial technology for delineating groundwater potential zones in Doddahalla watershed of Chitradurga district, India. *The Egyptian Journal of Remote Sensing and Space Sciences*. **19**: 223–234.

Jansen, H., Hengsdijik, H., Dagnachew Legesse, Tenalem Ayenew, Hellegers, P. & Spliethoff, P. (2007). Land and Water resource assessment in the Ethiopian Central Rift Valley; Project: ecosystems for water, food & economic development in the Ethiopian Central Rift Valley. Wageningen, Alterra, Alterra rapport 1587.

Jhariya, D.C., Kumar, T., Gobinath, M., Diwan, P. and Kishore, N. (2016). Assessment of Groundwater Potential Zone Using Remote Sensing, GIS and Multi Criteria Decision Analysis Techniques. *Journal of Geological Society of India*. **88**: 481–492.

Kolawole, M.S., Ishaku, J.M., Daniel, A., & Owonipa, O.D. (2016). Lineament Mapping and Groundwater Occurrence within the Vicinity of Osara Dam, Itakpe-Okene area, North Central Nigeria, Using Landsat Data. *Journal of Geosciences and Geomatics*. **4**(3): 42–52.

Kumar, P., Herath, S., Avtar, R. & Takeuchi, K. (2016). Mapping of groundwater potential zones in Killinochi area, Sri Lanka, using GIS and remote sensing techniques. *Sustain. Water Resour. Manag*. **2**:419–430.

Liu, C. (2016). Analysis of Sentinel-1 SAR data for mapping standing water in the Twente region. Unpublished MSc Thesis, Twente University, Geo-Information Science & Earth Observation, Enschede, Netherland.

Lwina, A., Myint, Khaing, M.M. (2012). Geomorphology identification and its Environmental impacts analysis by optical and radar sensing techniques. *International Archives of the Photogrammetry, Remote Sensing and Spatial Information Sciences*, XXXIX-B8, 2012 XXII ISPRS Congress, 25 August – 01 September 2012, Melbourne, Australia.

Makineci, H.B. & Karabork, H. (2016). Evaluation Digital Elevation Model Generated by Synthetic Aperture RADAR Data. *The International Archives of the Photogrammetry, Remote Sensing and Spatial Information Sciences*. **XLI-B1**: 57–62.

Mansaray, L.R., Huang, W., Zhang, D., Huang, J., & Li, J. (2017). Mapping Rice Fields in Urban Shanghai, Southeast China, Using Sentinel-1A and Landsat 8 Datasets. *Remote Sens*. **9**: 257; doi:10.3390/rs9030257.

Martinis, S. & Rieke, C. (2015). Backscatter analysis using multi-temporal and multi-frequency SAR Data in the Context of Flood Mapping at River Saale. *Journal of Remote Sensing*. **7:** (5): 7733–7752.

Mattia, F., (2011). GMES Sentinel-1 soil moisture retrieval algorithm development, European Space Agency contract n. 4000101352/10/NL/MP/ef, Final Report, November 2011.

Mbulisi, S., Timothy, D., Khoboso, S. & Samuel, A. (2015). Operational applications of remote sensing in groundwater mapping across sub-Saharan Africa. *Transactions of the Royal Society of South Africa*. **70** (2) :173–179.

Meijerink, A.M.J. (2007). *Remote sensing Applications to Groundwater*. UNESCO, Paris, 311 pp.

Melis, M.T., Dessi, F., Loddo, P., MantiaC. La., Pelo, S. Da., Deflorio, A.M., Ghiglieri, G., Biniyam Tesfaw, Kalegele, K. and Mwasi, B. N. (2017). An Application Based on Crowd-Generating Data Using Sentinel2 Imagery. *International Archives of the Photogrammetry, Remote Sensing and Spatial Information Sciences*. **XLII-4** (W2): 121–127.

Moore, G.K. (1982). Groundwater Applications of Remote sensing. United States of Geological Survey, Open-File Report, 82–240.

Mwega, W.B, Bancy, M.M., Mulwa, J.K. and G. M. Kituu, G.M. (2013). Identification of Groundwater Potential Zones using Remote Sensing and GIS in Lake Chala Watershed, Kenya. *Mechanical Engineering Conference on Sustainable Research and Innovation*. **5**: 42–46.

Navarro, A., Rolim, J., Miguel, I., Catalao, J., Silva, J., Painho, M & Vekerdy, Z. (2016). Crop Monitoring Based on SPOT-5 Take-5 and Sentinel-1A Data for the Estimation of Crop Water Requirements. *Remote Sens*. **8** (525): 1–20.

Ng, W., Rima, P., Einzmann, K., Immitzer, M., Atzberger, C. & Eckert, S. (2017). Assessing the Potential of Sentinel-2 and Plliades data for the Detection of Prosopis and Vachellia spp. in Kenya. **9** (74).

Nizalapur, V. (2008). Land cover classification using multi-source data fusion of Envisat- ASAR and IRS P6 LISS-III satellite data, a case study over tropical moist deciduous forested regions of Karnataka, India. *The International Archives of the Photogrammetry, Remote Sensing and Spatial Information Sciences*. **36** (6): 78–96.

Oh, H., Kim, Y., Choi, J., Park, E. & Lee, S. (2011). GIS mapping of regional probabilistic groundwater potential in the area of Pohang City, Korea. *Journal of Hydrology*. **399**: 158–172.

Oromia Water Works Design and Supervision Enterprise (2016). Impact Assessment of Water Resources Exploitation on Lake Ziway. Unpublished document, Addis Ababa, Ethiopia, 92 pp.

Oromia Water Works Design and Supervision Enterprise (2017). Oromia Irrigation Potential Assessment. Unpublished document, Addis Ababa, Ethiopia

Paloscia, S., Pettinato, S., Santi, E., Notarnicola, C., Pasolli, L., & Reppucci, A. (2013). Soil moisture mapping using Sentinel-1 images: Algorithm and preliminary validation. *Remote Sensing of Environment*. **134**:234–248.

Pinto, D., Shrestha, S., Babel, M.S. & Ninsawat, S. (2017). Delineation of groundwater potential zones in the Comoro watershed, Timor Leste using GIS, remote sensing and analytic hierarchy process (AHP) technique. *Appl Water Sci*. **7**:503–519.

potential zones in Doddahalla watershed of Chitradurga district, India. *The Egyptian Journal of Remote Sensing and Space Sciences*. **19**: 223–234.

Preeja, K.R, Joseph, S., Thomas, J. & Vijith, H. (2011). Identification of groundwater potential zones of a tropical river basin of Kerala, India using remote sensing and GIS techniques. *J. Indian Soc. Remote Sens*. **39**(1):83–94.

Rather, J.A., Andrabi, Z.R. (2012). Fuzzy Logic Based GIS Modeling for Identification of Ground Water Potential Zones in the Jhagrabaria Watershed of Allahabad District, Uttar Pradesh, India, *Int. Journal of Advances in Remote Sensing and GIS*. **1**(2): 218–233.

Robinson, C. (2007). Radar data contributes to groundwater exploration in the eastern Sahara. *The International Society for Optical Engineering.*

Rodriguez De Francisco, J.C. (2008). Preconditions for a payment for Environmental Services establishment at Central Rift Valley, Ethiopia. Wageningen University, Wageningen, Netherland.

Satty, T. L. (1980). Marketing applications of the analytic hierarchy process. *Management science*. **26**(7): 641–658.

Satty T.L. (2008). Decision making with the analytic hierarchy process. *Int. J. Services Sciences*. **1**(8):83–98.

Sanyal, J. and LU, X. X. (2004). Application of remote sensing in flood management with special reference to monsoon Asia. *Natural Hzards*. **33**: 283–301.

Sarmap (2009). *Synthetic aperture radar and sarscape - SAR guidebook*, 120 pp.

Seifu Kebede (2010). Groundwater in Ethiopia Occurrence, drought proofing and technology options. Addis Ababa University, department of Earth Sciences. Addis Ababa, Ethiopia.

Semere Solomon & Quiel, F. (2006). Groundwater study using remote sensing and geographic information systems (GIS) in the central highlands of Eritrea. *Hydrogeology*. **14**: 1029–1041.

Sentinel-1 User Handbook (2013). European Space Agency, GMES-S1OP-EOPG-TN-13-0001.

Shamuyarira, K.K. (2017). Determination of recharge and groundwater potential zones in Mhinga area, Unpublished MSc Thesis, Venda University, Venda, South Africa, 83 pp.

Sharma, M.P. & Kujur, A. (2012). ASTER DEM Based Studies for Geological and Geomorphological Investigation in and around Gola block, Ramgarh District, Jharkhand, India. *International Journal of Scientific & Engineering Research*. **3** (2).

Sivakumar, V. (2015). Geological, Geomorphological and Lineament mapping through Remote Sensing and GIS Techniques, in parts of Maduria, Ramanathapuram and Truchirappalli of Tmal Nadu. *International Journal of Geomatics and Geoscience*. **6**(3): 1669–1675.

Small D. & Schubert A. (2008). Guide to ASAR Geocoding.

Stehman, S. V. & Wickham, J. D. (2011). Pixels, blocks of pixels, and polygons: Choosing a spatial unit for thematic accuracy assessment. *Remote Sensing of Environment*. **115**(12): 3044–3055.

Strahler, A. N. (1952). Hypsometric (area-altitude) analysis of erosional topography. *Geological Society of America Bulletin*. **63**(11): 1117–1142.

Tamiru Alemayehu (1993). Preliminary analysis of the availability of groundwater in Ethiopia. *Ethiopian Journal of Science*. **16**(2):43–59

Tamiru Alemayehu (2006). Groundwater occurrence in Ethiopia, Addis Ababa University, Ethiopia, With the support of UNESCO.

Tao, T., Chocat, B., Liu, S. & Xin, K. (2009). Uncertainty Analysis of Interpolation Methods in Rainfall Spatial Distribution–A Case of Small Catchment in Lyon. *Water Resource and Protection*. **2**: 136–144

Tenalem Ayenew (1998). The hydrological system of the Lake District basin, Central Main Ethiopian Rift, Ph.D. Thesis. ITC Publication, 259 pp.

Tesfaye Chernet (1982). Hydrogeology of the Lakes Region, Ethiopia. Ethiopian Institute of Geological Surveys, Ministry of Mines & Energy. Addis Ababa, Ethiopia.

Tesfaye Chernet (1993). Hydrogeology of Ethiopia and water resource development. Ethiopian Institute of Geological Surveys, Ministry of Mines & Energy. Addis Ababa, Ethiopia.

Tesfaye Korme (1999). Lithologic and Structural mapping of the northeast Lake Ziway area, Ethiopian Rift with the help of Landsat TM data. *Ethiop. j. sci*. **22** (2): 151–174.

Tesfaye Tessema (2015). Ground Water Potential Evaluation Based on Integrated GIS and Remote Sensing Techniques, in Bilate River Catchment: South Rift Valley of Ethiopia.

American Scientific Research Journal for Engineering, Technology, and Sciences. **10**:85–120.

Tsegaye Abebe (2005). Geological map of northern main Ethiopia Rift, 1: 200,000 scales.

Ulaby, F.T., Dubois, P.C. & Van, J.Z. (1996). Radar mapping of surface soil moisture. *Journal of Hydrology*. **184**: 57–84.

Von, B., & Seifu Kebede (2012). Groundwater in Ethiopia, Features, Numbers and Opportunities. Springer, *Hydrogeology.*

Wagner, W., Bloschl, G., Pampaloni, P., Calvet, J. (2007). Operational Readiness of Microwave remote sensing of Soil moisture for hydrologic applications. *Nordic Hydrology*. **38** (1): 1–20.

Waikar, M.L. & Nilawar, A.P. (2014). Identification of Groundwater Potential Zone using Remote Sensing and GIS Technique. *International Journal of Innovative Research in Science, Engineering and Technology*. **3** (5): 12163–12174.

Werff, H. & Meer, F. (20016). Sentinel-2A MSI and Landsat 8 OLI Provide Data Continuity for Geological Remote Sensing. *Remote Sens*. **8** (883).

Wolfenden, E., Ebinger, C., Gezahegn Yirgu, Deino, A. & Dereje Ayale (2004). Evolution of the northern Main Ethiopian rift: Birth of a triple junction. *Earth Planet. Sci. Lett*. **224**: 213–228.

Workineh Haro, Daba Bulto, Mekonen Bekele, Desalegn Debelo, Muluken Kebede & Mohamed Edris (2014). Geology, Geochemistry, and Gravity survey of Asela area, Geological Survey of Ethiopia.

Zakaria, A., Abderrazak, E.H., Amine, J., Rachid, L., Lhou, M., Mohamed, A., Mohamed, Z. & Mostafa, B. (2017). Comparison of Landsat-8, ASTER and Sentinel 1 satellite remote sensing data in automatic lineaments extraction: A case study of Sidi Flah-Bouskour inlier, Moroccan Anti Atlas. *Advances in Space Research*. **60**: 2355–2367.

Zeinolabedini, M. & A. Esmaeily, A. (2015). Groundwater Potential Assessment using Geographic Information Systems and AHP method in Baft City, Kerman, IRAN. *The*

International Archives of the Photogrammetry, Remote Sensing and Spatial Information Sciences. **XL-1**(W5): 769–774.

Zhu, Z., He, X., Lu, G., Liu, Q. & Li, J. (2009). Ground Penetrating Radar Exploration for Ground Water and Contamination Progress In Electromagnetics Research Symposium Proceedings, Moscow, Russia, August 18–21, 2009. 1316-1320.

https://scihub.copernicus.eu, accessed on December 20, 2017.

https://sentinel.esa.int/web/sentinel/user-guides/sentinel-2-msi/data-formats, accessed on November 08, 2017.

https://sentinel.esa.int/web/sentinel/user-guides/sentinel-2-msi/resolutions/radiometric, accessed on November 23, 2017.

http://www.copernicus.eu, accessed on January 03, 2018.

Appendices

Annex I: Water point inventory data

Number	**Site name**	**Easting**	**Northing**	**Elevation** (m)	**Type**	**Depth** (m)	**Yield (l/sec.)**
1	Chefe Misoma	507412	880352	1782	BH	300	20
2	Chefe Misoma	507870	881052	1779	BH	300	20
3	Denba	509644	884775	1776	BH	300	20
4	Uhubo Berecha	500516	889860	1685	BH	202	18.5
5	Arsi University	515601	883040	2248	BH	250	
6	Arsi University	509904	883804	1775	BH	161	15.5
7	Arsi University	509630	883507	1784	BH	163	14.2
8	Ogolcho	501319	889352	1677	BH	75	
9		507412	880352	1777.9	BH	300	25
10	Kiyansho Kobota	492038	871194	1756	BH	190	
11		501227	889154	1689	BH	75	
12	Limat Abeba	503732	881064	1717	BH		2.5
13	Chefe Burkita	489715	867833	1790	BH		3.53
14	Kiansho	494507	874562	1728	BH	60	
15	Andode	504762	889812	1715	BH		
16	Korbeyi	503813	891279	1729	BH		
17	Sambaro (Dho)	498426	887206	1702	BH	37	
18	Dobdobo	496970	878361	1719	BH	80	
19	Kiansho	494507	874562	1728	BH	60	
20		507412	880352	1777.9	BH	300	25
21	Ogolcho	501886	887839	1672	BH		
22	Daho Hombo	496746	883403	1701	BH		
23	Sambaro	495878	886792	1664	BH		
24	Kobo Borera	495587	871329	1837	BH		
25	Abure	494121	867777	1880	BH		
26	Adere Lepho	488006	859301	1707	BH		
27	Golbe	495186	890646	1662	BH		
28	Korbeyi	503813	891279	1729	BH		
29	Andode	504762	889812	1715	BH		
30		509644	884775	1779	BH	300	25
31		510747	883663	1801.1	BH	300	25
32		507838	881591	1776.0	BH	300	25
33		508452	881365	1778.6	BH	300	25
34		500092	887644	1684	HDW		
35	Aba Tola	533613	849372	2827	HDW		0.25
36	Sambaro	496995	886709	1756	HDW	48	
37	Birkamanabernoto	506216	865501	2462	HDW		0.2

38	Dosota	506436	865302	2459	HDW		0.3
39	Dosha Safara	514052	874393	2527	HDW		0.3
40	North Assela	515709	882675	2279	HDW		0.26
41	Adematu	529539	867362	3079	SP		0.36
42	Awashu	532641	823308	3043	SP		1.5
43	Jiso	515829	827459		SP		1.6
44	Hayana	530881	828335	2929	SP		0.5
45	Hundeshine Minch	527059	834011	2725	SP		2
46	Bacho	527050	834014	2709	SP		0.5
47	Jalcho	527842	836531	2737	SP		0.63
48	Gena bontu	530189	837408	2893	SP		0.17
49	Mission Minch	525009	841183	2533	SP		1
50	Burkitu Minch	524630	843700	2483	SP		2
51	Sof-umer	534295	847693	2874	SP		1.8
52	Burkah	529716	847960	2660	SP		1.8
53	Weshe	525449	848065	2499	SP		1
54	Burka waraaba	533985	848439	2858	SP		2.3
55	Mada Burka	509010	881446	1782	SP		3
56	Chursa	504116	822698	3285	SP		0.13
57	Konsa	508975	822901	3020	SP		0.26
58	Tabala	521491	859241		SP		0.7
59	Burkitu	511343	877889	2235	SP		0.17
60	Selale	529111	864002	2912	SP		1
61	Burkitu	532214	853942	2783	SP		1.6
62	Tabala	521491	859241		SP		0.72
63	Sirba Minchi	525095	841183	2533	SP		15

Annex II: Description of geological units in the study area

Symbol	Geological unit	Description
Tv7	Pliocene trachyte	The mountains of eastern highlands of Ethiopia are made up of this information. The mountains are Chilalo, Badda, Kakka and Kubsa. These rocks are massive and slightly weathered
Qa	Alluvial	Mainly terrace gravel, sand and silt associated locally with clay
Tv4	Highland basalt	These are central eruptions and exposed on top of upper pyroclasts. They are exposed around Bekoji, northeast of Meraro, Gobesa area, and northeast of Digelu areas. These lava flows form large plateau areas and are younger fresh basalts.

Ql	Lacustrine sediment	They consist of alternating fine and course beds, but they are predominantly fine to medium grained course. It has an average thickness of 40 to 50 meters.
Tv6	Pliocene basalt flow	The Pliocene basalts are exposed on the highland areas, restricted to the foot slopes of mountain peaks. They are exposed below Chilalo, Kaka, and Galema mountains. The basalts are fresh, compact, massive, and dense, usually grey to dark grey in color.
Qwbp, Qwh, Qwbh	Basalts of the Rift floor	The type of volcanic activity in the Wonji Group was the eruption from fissures of Pleistocene basalts (Qwbp) and recent basalts (Qwbh). The bulk of these late basalts are concentrated in the Wonji fault belt. These basalts are clearly controlled by extensional fractures. The recent basalt flows have up to 100 meters thick and occur east of Lake Ziway in the study area. Other manifestations of recent and sub recent basaltic volcanism are explosion craters and basaltic hyalloclastites (Qwh). These basalts are alkaline or transitional, mostly mildly alkaline.
Qwpu	Pumice and unwelded tuffs	They occur partly in mountains north of Lake Ziway. The rock is characterized by a high inter granular permeability which becomes highest when sorted.
Qwa	Rhyolitic and trachytic lava domes and flows	Show discrete east–west alignment and may follow transverse faults.

Annex III: Mean monthly annual rainfall for the last 30 years of the study area (1987 −2016)

Year	Jan	Feb	Mar	Apr	May	Jun	Jul	Aug	Sep	Oct	Nov	Dec
1987	2.9	36.1	74.5	98.4	138.5	67.1	106.2	111.0	70.1	22.6	1.2	8.0
1988	16.1	50.1	22.0	117.4	51.9	105.9	229.2	158.8	150.4	68.4	1.4	1.7
1989	3.5	33.3	88.4	139.3	29.6	121.4	143.8	165.8	102.5	36.7	5.2	36.5
1990	45.9	135.2	84.9	91.9	34.9	100.6	161.1	137.5	92.5	7.7	8.6	1.5
1991	4.0	44.0	148.4	35.2	56.1	79.0	171.8	125.1	73.0	13.2	0.9	17.1
1992	36.6	62.8	56.9	67.7	48.6	73.0	147.1	189.1	111.6	65.2	18.4	17.8
1993	22.4	44.0	15.4	144.2	136.9	53.6	155.8	179.3	109.5	71.2	0.9	5.7
1994	0.1	3.5	53.6	61.1	62.8	166.4	172.8	144.1	106.1	2.4	22.0	3.9
1995	0.0	26.8	108.2	148.7	73.1	94.3	165.0	164.4	100.6	18.4	0.2	29.4
1996	46.5	6.2	108.0	59.6	156.0	143.7	140.2	139.2	106.2	13.1	3.3	1.7
1997	22.4	7.1	109.0	132.9	48.7	98.8	176.5	98.1	102.7	86.4	32.5	0.8
1998	32.5	50.2	70.8	67.8	77.3	83.6	146.8	225.7	129.7	110.2	12.5	0.1
1999	6.7	7.7	46.6	24.0	48.0	91.4	137.4	108.4	84.3	182.7	5.7	0.3
2000	0.6	0.7	10.5	83.2	119.6	106.0	146.6	145.1	160.0	67.2	56.6	3.2
2001	2.0	25.0	167.6	25.6	185.8	157.7	165.0	225.5	117.5	14.0	4.1	1.1
2002	38.4	41.5	79.8	47.9	66.4	93.5	109.0	176.3	76.8	3.8	0.0	26.7

2003	20.0	38.7	81.7	128.4	32.2	104.3	174.6	143.2	126.0	7.2	3.8	29.7
2004	37.2	1.1	45.6	124.7	31.6	100.2	127.4	103.6	140.5	75.1	6.9	11.1
2005	51.9	26.7	77.4	122.4	107.9	63.1	108.7	92.3	90.4	23.9	23.3	1.1
2006	11.9	26.6	59.6	115.8	69.8	109.2	175.4	124.5	80.2	42.0	0.7	12.8
2007	18.3	29.5	57.5	85.4	118.1	148.9	184.4	150.6	101.9	30.3	21.6	0.1
2008	4.2	2.5	18.8	55.5	101.2	106.4	208.5	204.4	97.0	84.8	61.7	0.4
2009	40.0	82.0	66.4	67.7	86.5	71.0	160.0	164.8	107.9	58.4	13.4	17.0
2010	11.0	96.1	106.5	111.5	108.4	101.8	223.8	132.6	132.7	8.8	5.8	9.9
2011	10.5	15.6	72.1	59.9	123.8	98.4	155.2	143.5	124.0	1.7	19.2	1.6
2012	0.8	8.7	30.8	98.9	47.2	94.7	210.4	170.6	149.4	17.2	5.7	3.8
2013	10.6	0.7	97.5	61.0	98.2	76.9	203.8	132.4	80.7	75.1	15.3	2.2
2014	2.7	24.8	66.4	54.3	95.7	56.2	148.6	159.4	124.1	114.0	10.0	1.9
2015	1.8	1.7	26.7	50.3	87.4	125.3	107.1	99.4	92.8	34.6	15.8	7.6
2016	12.4	10.0	36.8	138.3	96.4	97.9	116.3	87.0	86.5	48.7	18.2	7.3
Average	17.1	31.3	69.6	87.3	84.62	99.7	159.3	146.7	107.6	46.8	13.2	8.7

Annex IV: Sentinel-2A band description

Bands	**Central Wavelength (nm)**	**Band width (nm)**	**Resolution (m)**
Band 1- Coastal aerosol	443	20	60
Band 2- Blue	490	65	10
Band 3- Green	560	35	10
Band 4- Red	665	30	10
Band 5- Vegetation Red Edge	705	15	20
Band 6- Vegetation Red Edge	740	15	20
Band 7- Vegetation Red Edge	783	20	20
Band 8- NIR	842	115	10
Band 8A- Vegetation Red Edge	865	20	20
Band 9- Water vapor	945	20	60
Band 10- SWIR Cirrus	1375	30	60
Band 11- SWIR	1610	90	20
Band 12- SWIR	2190	180	20

Annex V: Land-use/Land-cover classification accuracy

	Fa	Sh	B	G	Fo	Se	We	Wa	Total	U. A
Fa	60	1	2	3	1	2	1	0	70	85.71
Sh	1	35	2	0	2	0	0	0	40	87.50
B	2	2	28	1	0	1	1	0	35	80.00
G	2	0	1	27	0	0	2	0	32	84.38
Fo	1	4	0	0	23	0	0	0	28	82.14
Se	2	0	1	2		20	0	0	25	80.00
We	1	0	0	2	0	0	22	0	25	88.00
Wa	0	0	0	0	0	0	0	20	20	100.00

Total	69	42	34	35	26	23	26	20	275	Correctly classified=235
P. A	86.96	83.33	82.35	77.14	88.46	86.96	84.62	100		
Over all accuracy = 85.45%; $K_{hat=}$ 0.83										
P.A = Producer Accuracy; U. A= User Accuracy; Fa= Farmland; Sh= Shrubland; B= Bare-land; G= Grassland; Fo= Forest; Se= Settlement; Wetland; Wa= Waterbody.										

Annex VI: Sentinel-1A SAR Product description

Mission: Sentinel-1A

Product: S1A_IW_GRDH_1SDV_20170104T030918_20170104T030943_014676_017E01_1492

Product type: GRD

Acquisition mode: IW

Description: Sentinel-1 IW Level-1 GRD

Processed time: 04-JAN-2017 05:04:02.639999

Processing system identifier: ESA Sentinel-1 IPF 002.72

Orbit cycle: 98

Data take identifier: 97793

Pass: descending

Radar frequency: 5.405. GHz

Calibration factor: 99999.0

Polarization: VH

Band names: Amplitude VH

First line time: 04-JAN-2017 03:09:18.539615.

Last line time: 04-JAN-2017 03:09:43.537694

DECLARATION

I the undersigned declare that this thesis is my original work and has not been presented for a Degree in any other university and that all sources of materials used for the thesis have been duly acknowledged.

Wondifraw Nigussie Mekuria

Signature ________________________ Date_______________________

School of Earth Science

June, 2018

This thesis has been submitted for examination with my approval as university advisor.

Advisor:

Dr. Binyam Tesfaw

Signature __________________Date___________________

Co-Advisor

Dr. Tilahun Azagegn

Signature __________________Date___________________